Master's Thesis

SURFACE MODIFICATION OF SWRO MEMBRANE WITH ZWITTERIONIC CHEMICAL MPC VIA SI-ATRP FOR ENHANCING ANTI-FOULING CAPABILITY

Jihun Park

Department of Urban and Environmental Engineering
(Environmental Science and Engineering)

Graduate School of UNIST

2019

SURFACE MODIFICATION OF SWRO MEMBRANE WITH ZWITTERIONIC CHEMICAL MPC VIA SI-ATRP FOR ENHANCING ANTI-FOULING CAPABILITY

Jihun Park

Department of Urban and Environmental Engineering
(Environmental Science and Engineering)

Graduate School of UNIST

SURFACE MODIFICATION OF SWRO MEMBRANE WITH ZWITTERIONIC CHEMICAL MPC VIA SI-ATRP FOR ENHANCING ANTI-FOULING CAPABILITY

A thesis/dissertation
submitted to the Graduate School of UNIST
in partial fulfillment of the
requirements for the degree of
Master of Science

Jihun Park

7.12.2019 of submission
Approved by

_____

Advisor

Young-Nam Kwon

SURFACE MODIFICATION OF SWRO MEMBRANE WITH ZWITTERIONIC CHEMICAL MPC VIA SI-ATRP FOR ENHANCING ANTI-FOULING CAPABILITY

Jihun Park

This certifies that the thesis/dissertation of Jihun Park is approved.

7.12.2019 of submission

_____

Advisor: Young-Nam Kwon

_____

Changsoo Lee : Thesis Committee Member #1

_____

Jae Weon Cho : Thesis Committee Member #2

Abstract

Reverse osmosis (RO) is a typical desalination process that uses semi-permeable membranes for separating dissolved materials in solution. The membrane passes liquids and some of ions, however rejection is most dissolved materials. It is also most promising efficient ways for the desalination of sea water and brine by reverse osmosis (RO) process. Although RO applicable on the various liquid solution, the largest application of RO is in water-based systems. Until now, the RO membrane process has proven to be an economically feasible separation technology for the purification of surface water contaminated with heavy metals, insecticides and other contaminants as well as seawater desalination. However, there is still a need for RO processes, such as reducing operating energy, extending membrane cleaning frequency, optimizing membrane modules, RO system configuration design, and understanding of the separation mechanism of the RO filtration process.

In this work, using commercially available two thin film composite (TFC) SWRO membranes were modified by surface initiated atom transfer radical polymerization (si-ATRP) method to graft target zwitterion chemical 2(methacryloyloxy) ethyl phosphorylcholine (MPC) brushes poly-MPC (PMPC) applied to the surface of membranes for enhancing fouling resistance. For confirming successful surface modification of PMPC, analyzing surface properties of membranes related to chemical structure via attenuated total reflectance-Fourier transform infrared spectroscopy (ATR-FTIR), atomic composition ratio of each element via X-ray photoelectron spectroscopy (XPS), morphology of membrane surface via scanning electron microscopes (SEMs), and hydrophilicity change of membrane surface via contact angle measurement based on a salting in/out effect on the surface of membranes, respectively. Pure membrane and MPC modified membranes RO filtration performance test conducted via RO filtration system with four cells are connected in series at the artificial seawater feed tank condition. Fouling resistance and cleaning efficiency test of membranes performance test also conducted via same RO filtration system with two model foulants, sodium alginate and bovine serum albumin after 30 hours compaction step.

Because of the presence of zwitterionic chemical MPC in the composite coating membrane, MPC modified SWRO membranes are believed to be a key basis for increasing surface hydrophilicity and thus exhibiting improved anti-contamination effectiveness for both two model foulants at the artificial seawater solution condition. Overall, these in this study imply that the successful surface modification of zwitterion MPC on TFC SWRO membranes surfaces is prospective opportunities for seawater desalination industrial area.

Contents

Abstract……i

Contents……ii

List of Figures……iii

List of Tables……iv

Chapter 1. Introduction……1

1.1 Objective of this study……1

1.2. Research background……1

1.2.1 Water shortage problem……1

1.2.2 Zwitterionic polymers……3

1.2.3 Target zwitterionic chemical MPC……4

Chapter 2. Materials and methods……5

2.1 Materials……5

2.2 Surface coating method: si-ATRP……6

2.3 Characterization of membranes……7

2.3.1 Attenuated total reflectance-Fourier transform infrared spectroscopy (ATR-FTIR)...7

2.3.2 X-ray photoelectron spectra (XPS)……7

2.3.3 Scanning electron microscopy (SEM)……7

2.3.4 Water contact angle……7

2.4 Performance evaluation of membranes……8

2.4.1 Membrane RO filtration performance evaluation……8

2.4.2 Fouling performance evaluation……10

Chapter 3. Results and discussions……11

3.1 Attenuated total reflectance-Fourier transform infrared spectroscopy (ATR-FTIR)…...11

3.2 X-ray photoelectron spectra (XPS)……..…..13

3.3 Scanning electron microscopy (SEM)…….…..…...16

3.4 Water contact angle……...18

3.5 Membrane performance evaluation……..23

3.5.1 Fouling performance test: Compaction step……..23

3.5.2 Fouling performance test: 2 sets fouling test……27

Chapter 4. Conclusions…….……..33

Reference…….……..34

List of Figures

Figure 1. Distribution of water on the earth

Figure 2. Chemical structure of zwitterionic chemical MPC

Figure 3. Schematic diagram of the chemical reaction for preparing zwitterionic chemical MPC coated SWRO membranes

Figure 4. Schematic of the reverse osmosis (RO) filtration system with series connected flow membrane cells

Figure 5. FT-IR spectra of virgin, BIBB-initiated, MPC-modified (a) DOW and (b) Toray membranes

Figure 6. XPS wide scan spectra of (a) Virgin and (b) MPC-modified DOW membrane with the enlarged P peak

Figure 7. XPS wide scan spectra of (a) Virgin and (b) MPC-modified Toray membrane with the enlarged P peak

Figure 8. Surface morphology images of virgin, BIBB initiated, MPC modified DOW membrane. (a), (b) virgin membrane, (c), (d) BIBB initiated membrane and (e), (f) MPC modified membrane each.

Figure 9. Surface morphology images of virgin, BIBB initiated, MPC modified Toray membrane. (a), (b) virgin membrane, (c), (d) BIBB initiated membrane and (e), (f) MPC modified membrane each.

Figure 10. Surface contact angle of virgin, BIBB initiated and MPC modified DOW membranes. (a), (c), (e) are drops of DI water contact angle of virgin, BIBB initiated and MPC modified respectively. (b), (d), (f) are drops of artificial seawater contact angle of virgin, BIBB initiated and MPC modified respectively.

Figure 11. Surface contact angle of virgin, BIBB initiated and MPC modified Toray membranes. (a), (c), (e) are drops of DI water contact angle of virgin, BIBB initiated and MPC modified respectively. (b), (d), (f) are drops of artificial seawater contact angle of virgin, BIBB initiated and MPC modified respectively.

Figure 12. Diagram of "salting-in effect" on MPC-modified membrane in the artificial seawater solution

Figure 13. Drop contact angle of (a) DI water, (b) artificial seawater on DOW membranes.

Figure 14. Drop contact angle of (a) DI water, (b) artificial seawater on Toray membranes.

Figure 15. Flux decline tendency of virgin and MPC modified SWRO membranes during 30 hours membrane compaction step in artificial seawater feed tank condition for with sodium alginate test

Figure 16. R (%), salts rejection, data of virgin and MPC modified SWRO membranes during 30 hours membrane compaction step in artificial seawater feed tank condition for with sodium alginate test.

Figure 17. Flux decline tendency of virgin and MPC modified SWRO membranes during 30 hours membrane compaction step in artificial seawater feed tank condition for with BSA test

Figure 18. R (%), salts rejection, data of virgin and MPC modified SWRO membranes during 30 hours membrane compaction step in artificial seawater feed tank condition for with BSA test.

Figure 19. Flux decline tendency of virgin and MPC modified membrane during total fouling performance test with 30 ppm sodium alginate in artificial SW feed tank conditions

Figure 20. R (%), salts rejection, data of virgin and MPC modified SWRO membranes during total fouling performance test with 30 ppm sodium alginate in artificial SW conditions

Figure 21. Flux decline tendency of virgin and MPC modified SWRO membrane during total fouling performance test with 10 ppm bovine albumin serum in artificial SW feed tank conditions

Figure 22 R (%), salts rejection, data of virgin and MPC modified SWRO membranes during total fouling performance test with 10 ppm bovine albumin serum in artificial SW conditions

Figure 23. Nomalized flux tendency and FR (%), flux recovery, of virgin and MPC modified SWRO membrane during 1st and 2nd anti-fouling performance test with 30 ppm sodium alginate in artificial SW condition

Figure 24. Nomalized flux tendency and FR (%), flux recovery, of virgin and MPC modified SWRO membrane during 1st and 2nd anti-fouling performance test with 10 ppm bovine albumin serum in artificial SW condition

List of Tables

Table 1. Specific composition and concentration for each salts of 'Standard ASTM D1141-98' artificial seawater condition

Table 2. Comparative atomic concentration ratio (C, N, O, and P) of Virgin and MPC modified DOW membrane.

Table 3. Comparative atomic concentration ratio (C, N, O and P) of Virgin and MPC modified Toray membrane.

Chapter 1. Introduction

1.1. Objective of this study

The overall objective of this study aims to investigate the enhanced anti-fouling capability of surface modified commercially available polyamide based TFC SWRO membranes with zwitterionic chemical MPC against the pure membrane through the surface modification by surface-initiated atom transfer radical polymerization (si-ATRP), then increased in surface hydrophilicity that suitable to biofouling water condition. That is why the water molecules formation to hydration layer onto the membrane, so decreasing the driving polarity of surface with foulant. The analytical method for analyzing physical and chemical properties of the membrane surface, MPC considered the surface of the synthesis to be synthetic. Consequently, this study can suggest the opportunities for seawater desalination industrial area.

1.2. Research background

1.2.1. Water shortage problem

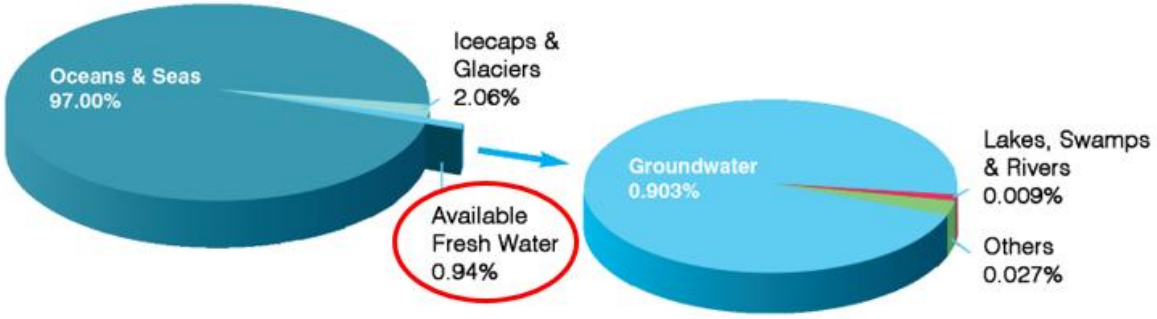

Figure 7. Distribution of water on the earth

97% of the global water is seawater, then freshwater accounts for only 3%. Except for glaciers, the actual water available is less than 1%. As the water shortage crisis more deeper, the seawater desalination project that makes seawater freshwater is promising. So, seawater have become the most important sources of drinking water in the future. Global warming is expected to account for about 20% of the global water shortage of this century. Global warming has predicted to change the world's

precipitation patterns, dissolve mountain glaciers, and exacerbate extreme droughts and floods. The world's water consumption is eight times earlier than the population growth rate in the last century, doubling and growing rapidly over the next decades. Still, the ready-to-use fresh water is a finite resource, less than 1% of the world's water. In addition, water and population are ubiquitous around the world. Dry and semi-arid zones account for only 2% of the total surface runoff, but account for 40% of the world's land area and account for half of the world's poor. Finally, our existing freshwater resources are under serious threat from over development, pollution, and global warming. Given this trend, it is one of the biggest challenges of the 21st century to provide equitably sufficient water resources for agriculture, industry and human consumption.

The physical evidence of water scarcity is growing globally and equally affects both rich and poor countries. There are about 3 billion people in the water shortage (more than 40% of the world population) and this situation can get worse if the current growth trend continues. Political conflicts due to water shortages, extinction of freshwater species and deterioration of aquatic ecosystems are causing millions of deaths each year. Almost half of all wetlands have already been damaged and the dam has severely altered the flow of about 60% of the world's major river basins. There is no absolute amount of water shortage. It is common in both dry and humid climates. Rather, it is a relative concept that compares water availability to actual use. In deserts, for example, water demand is low and water is not classified if it is small. However, if there is a serious strain of population, excessive pollution, or a level of unsustainable consumption, shortages may occur in water-rich areas. To summarize, this type of physical water shortage affects about one-fifth of all continents and the world's population. In the United States and Europe, we use an average of 200 to 600 liters of water a day compared to 20 liters, which is considered the minimum daily requirement for beverage, laundry, cooking and hygiene. This level of unsustainable consumption has resulted in local water scarcity and a drastically changing freshwater ecosystem. Cities like Los Angeles, San Diego, Las Vegas desert, and millions of farmland supply American giant Colorado rivers are now dry before reaching the sea. As a result, the Colorado River Delta, which once supported the life of an abundance of flora and fauna, is now declining significantly.

Economic water shortages occur when water resources are abundant in water use, but insufficient infrastructures or financial resources prevent people from accessing the water they need. This dilemma afflicts 1.6 billion people around the world, especially the poor in rural areas, especially in Africa. Therefore, additional investment in the water sector in developing countries can play a transformative role in poverty alleviation. For example, slum dwellers pay 5 to 10 times more per unit of water than people who use tap water. In rural homes, women and children are often not as safe as water. Agriculture accounts for 70% of global water consumption and up to 95% in some developing countries. It accounts for more than 40 percent of the world's harvest, 20 percent of irrigated agricultural land, and has a significant impact on the world's water availability and the future of food security. The world population

is projected to increase by 50% by 2050. World economic development and income growth will increase per capita food consumption and water consumption. The use of agricultural water will increase dramatically, especially as more people in developing countries are able to buy a variety of foods, including meat and vegetables. One kilogram of wheat requires ten times more water to raise one kilo of beef.

The global water situation is likely to be dark due to constant population growth, increased per capita consumption and projected climate change. Because it is a very local problem, which is determined by the climate and demographic factors of the water scarce region, a single solution can not solve all of the world's water shortages. However, improvements in management, water-efficient technologies, and support for the world's most vulnerable nations and ecosystems will play a leading role. According to the World Water Council, supported by the United Nations, a global investment of $ 100 billion a year is needed to cope with water shortages. This amount of investment motivation is essential to the future of human happiness and economic development in all countries of the world.

1.2.2. Zwitterionic polymers

Basically, zwitterion meaning is a molecule with two or more functional groups at least one has a positive and another has a negative charge, so zwitterinoic polymers also are polymers possessing both positively and negatively charged functional groups, such as these chemicals. Also, the water molecules form a structured hydration layer structure on the membrane, which in turn reduces the interaction between the surface and the stain and tereby interferes with the attachment of molecules and particles, so that the hydrophilic surface is not affected by the bio-adhesion of the water condition.

Therefore, zwitterionic polymers was thought to valuable exploring for anti-fouling target chemical for membranes. The type of expanded steric effect on membrane contamination under seawater condition.

1.2.3. Target zwitterionic chemical: MPC

In this study, MPC (2-Methacryloyloxyethyl phosphorylcholine) selected from a number of zwitterionic chemical, because MPC has been already widely applied in surface coating fields such as biomaterials with excellent biocompatibility and it can not cause tissue inflammation and infection. In addition, MPC has a higly hydrophilic sensory phosphorylcholine functional group, which can resist protein adsorption and bacterial adhesion. Thus MPC-based polymers have great potential for development as a hydrophilic, biocompatible and anti-fouling surface for SWRO membrane. This research is the first time MPC has been applied to SWRO membranes surface coating.

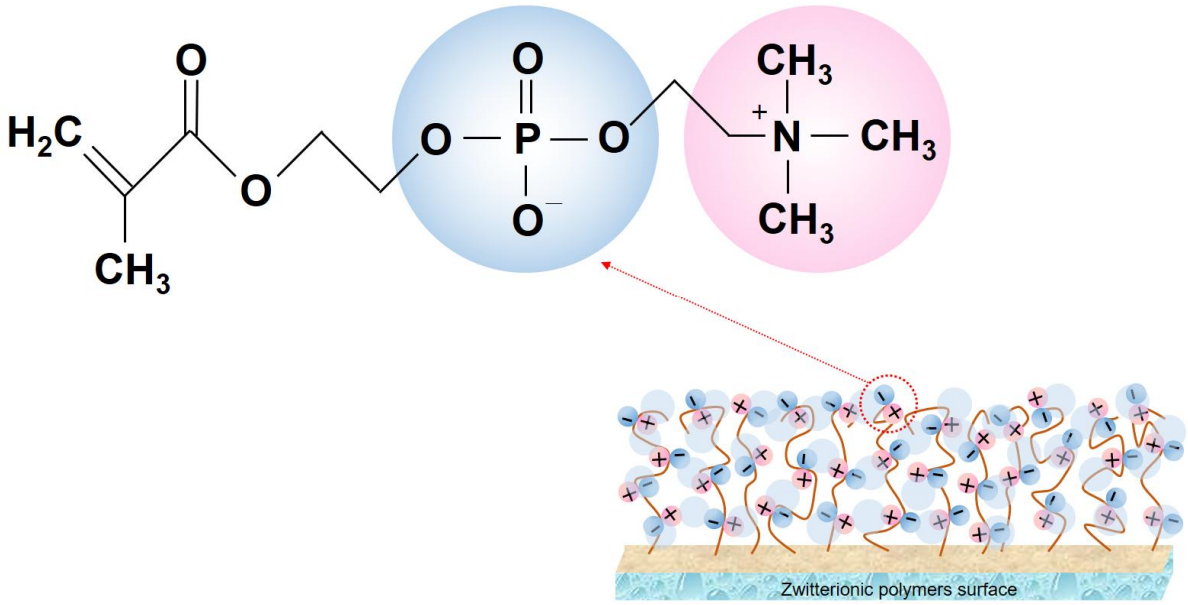

Figure 8. Chemical structure of zwitterionic chemical MPC

Chapter 2. Materials and Methods

2.1. Materials

Prepare commercially available polyamide (PA) based seawater reverse osmosis membrane SW30ULE-400i that was purchased from DOW FILMTEC™ and SHF was purchased from Toray Chemical Korea Inc. They are thin film composite (TFC) SWRO membrane having a selective polyamide surface layer polymerized at the interface of a polysulfone sub layer supported by a nonwoven fabric. Target zwitterionic chemical 2-Methacryloyloxyethyl phosphorylcholine (MPC, molecular weight 295.27) was purchased Sigma-Aldrich Chemical (Korea). For using to make artificial seawater based on 'Standard ASTM D1141-98', Sodium chloride (NaCl), Strontium chloride hexahydrate ($SrCl_2 \cdot 6H_2O$), Sodium fluoride (NaF) was purchased from DAEJUNG Chemicals (Korea), Sodium sulfate, ACS reagent (Na_2SO_4), Calcium chloride ($CaCl_2$), Potassium chloride (KCl), Sodium bicarbonate ACS reagent ($NaHCO_3$), Boric acid (H_3BO_3) was purchased from Sigma-Aldrich Chemical (Korea), Magnesium chloride hexahydrate ($MgCl_2 \cdot 6H_2O$) was purchased from SAMCHUN Chemical and Potassium bromide (KBr) was purchased from JUNSEI Chemical. For membrane surface coating, Methanol was purchased from SK Chemicals, Triethylamine, α-Bromoisobutyryl bromide (BIBB), *N*,*N*,*N*′,*N*″,*N*″′-Pentamethyldiethylenetriamine (PMDETA), Copper(I) Bromide (Cu(I)Br) was purchased from Sigma-Aldrich Chemical (Korea). For membrane RO filtration fouling performance test, Sodium alginate was purchased from JUNSEI Chemical and Bovine serum albumin was purchased from Sigma-Aldrich Chemical (Korea). Milli-Q water (18 MΩ resistivity, Millipore®, Merck Millipore, Germany) is used as a solvent for soaking the membrane samples and for preparing aqueous experiment solutions. All the materials were used without further purification steps.

2.2. Surface coating method: si-ATRP

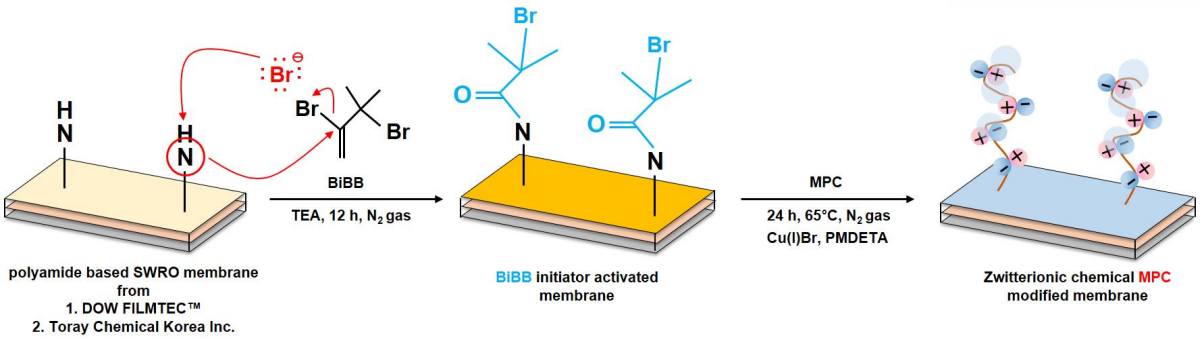

Figure 9. Schematic diagram of the chemical reaction for preparing zwitterionic chemical MPC coated SWRO membranes

The above schematic diagram describes si-ATRP (surface initiated – Atom Transfer Radical Polmerization) in grafting method for surface modification of TFC SWRO membranes with zwitterionic chemical MPC. Firstly, preparing commercial TFC SWRO membranes that has been socked sufficiently in to the flowing DI water bath during at least 24 hours. Then fixing the cut membranes (6.0 cm x 10.0 cm) on the stainless tray with 300 mL MeOH as a solvent in the globe box for 30 min N_2 gas purging. Put in 2.25 mL Triethylamine (TEA) as a base also catalyst and then 1.95 mL α-Bromoisobutyryl bromide (BIBB) as a initiator into the tray for initiating membrane surface with Br during at least 12 hours. To sum up the mechanism of this step, firstly the amide group on membrane surface attack the carbon with double bond on BIBB, then bromide anion leaving the BIBB. This bromide anion re-attack the hydrogen of amide group on membrane surface, so membrane surface is activated with BIBB initiator. From this step hydrobromide (HBr) by product are created. That is why using TEA as a base and catalyst for creating trimethylamine hydrobromide ($Et_3N{\cdot}H^+Br^-$) by product that regardless of the zwitterionic chemical MPC modification on membrane. At next step, washing these Br initiated SWRO membrane with MeOH for cleaning by product and preparing zwitterionic polymer MPC coating ATRP method step. Then put in solution prepared in advance with 0.3 mL (4.8 mM) PMDETA as a ligand, 0.151 g (3.5 mM) Cu(I)Br as a catalyst and 0.31 (0.35 mM) MPC as a target coating material and react at 65°C during 24 hours. At lastly, wash the modified membrane within circulating DI water bath during 24 hours, after this step set vacuum freeze dried during 72 hours for analyzing membrane surface characterization.

2.3. Characterization of membranes

2.3.1 Attenuated total reflectance-Fourier transform infrared spectroscopy (ATR-FTIR)

The ATR-FTIR was used to identify the surface functional groups of membrane surface using a Nicolet 6700 spectrometer (Thermo Scientific, Waltham, MA, USA) including a flat plate germanium (Ge) ATR crystal. Omnic 8.1 software program was used to analyze the FTIR spectra wave lengths of 600 to 4000 cm^{-1} were measured for 64 scans per sample with a resolution of 4 cm^{-1}.

2.3.2 X-ray photoelectron spectra (XPS)

XPS (K Alpha, Thermo Fisher Scientific, USA) and a double focusing hemispherical analyzer were analyzed to estimate the atomic percent composition and ratio of carbon (C), nitrogen (N), oxygen (O), phosphorus (P) on membrane surface. The survey XPS spot area were measured approximately by a range from 0 to 1400 eV of electron binding energy with step size of 0.1 eV. From this study, the binding energy of C1s, N1s, O1s, P2s, P2p were detected at 283, 398, 533, 176 and 144 eV, respectively.

2.3.3 Scanning electron microscopy (SEM)

The S-4800 Hitachi devices was used to visualize the morphology image of membrane surface. Before taking the SEM images, pure membrane sample and performance tested membranes are set vacuum freeze dried during 72 hours for preparing. Also, all sample's images enlargement ratio was measured at 10.0 k and 50.0 k magnifications two times, respectively.

2.3.4 Water contact angle

The water contact angle was estimated for checking hydrophilicity change of membrane's surface after modification by using goniometer (Phoenix 300 Plus from Surface & Electro Optics Co. Ltd. Korea). In this study, uses SWRO membrane, all the samples contact angle were taken both pure DI water and artificial seawater (concentration is as same as feed tank condition) 3 um sessile drops method, respectively. For taking contact angles, 12 times different points of contact angle were measured for each membrane samples respectively. Also, before taking the contact angles, all samples are set vacuum freeze dried during 72 hours for preparing.

2.4. Performance evaluation of membranes

2.4.1 Membrane RO filtration performance evaluation

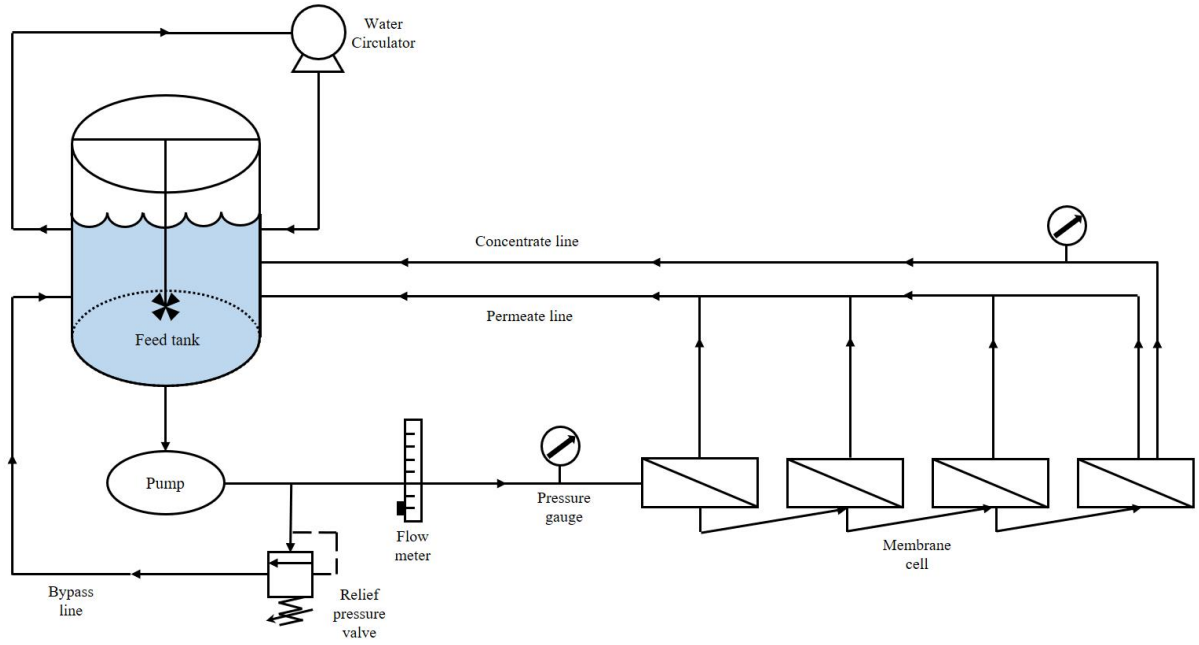

Figure 10. Schematic of the reverse osmosis (RO) filtration system with series connected flow membrane cells

As shown in Figure 4, membrane filtration experiments were conducted this lab scales filtration system with series connected flow 4 membrane cells with an effective active area of 60 cm^2 (6.0 cm x 7.5 cm). Each company membranes are set crossed at 4 membrane cells when evaluating performance test (for example: 1- pure Dow, 2- pure Toray, 3- MPC Dow, 4- MPC Toray). The feed tank was filled to 35 L with stock artificial seawater solution (Table 1.) at room temperature (25 ± 0.5 °C), the test conditions of applied pressure at 62.1 bar (900 psi) during whole step of filtration evaluation including stabilization and compaction steps. The feed tank temperature was controlled and maintained by water circulator and the flow meter was controlled at 3.3 ± 0.1 L/min flow rates by concentrate flowmeter. Also, when taking permeate sampling for calculating permeate water flux J_w ($Lm^{-2}h^{-1}$ or LMH), it was measured during 30 hours compaction step with 5 min in a Falcon tube per unit of effective membrane area and per unit time. The sampling time was measured at a short term in the early period when the flux was unstable, and the measurement was conducted by increasing the term as it tended to become more stable. In detailed, first of all, 30 hours compaction step was conducted to make the membrane which consists of polymer familiar to cell. Normalized permeate water flux was calculated as the flux of membranes divided by the initial permeate water flux at the last sampling point of compaction step. When calculating salt rejection regard as seawater ion was measured by conductivity from the

conducted permeate sampling and feed tank solution by calibrated conductivity meter (feed tank conductivity meter: Orion Star Conductivity Benchtop Meter, Thermo Fisher Scientific™, USA and permeate sampling conductivity meter: Ultrameter, Myron L® company, USA). Permeate water flux J_w and salt rejection were calculated using the following equations:

$$J_w = \frac{V}{A \cdot t \cdot \rho} \qquad (3.1)$$

$$R\ (\%) = \left(1 - \frac{C_{permeate}}{C_{feed}}\right)\ X\ 100 \qquad (3.2)$$

where:

J_w : Permeate water flux (L/m^2 h)

V : Permeate weight (kg)

A : Effective membrane area (m^2)

t : Time (hour)

ρ : Density of water (g L^{-1})

Table 1. Specific composition and concentration for each salts of 'Standard ASTM D1141-98' artificial seawater condition

Standard ASTM D1141-98	
Composition	Concentration (g/L)
NaCl	24.53
$MgCl_2$	5.2
Na_2SO_4	4.09
$CaCl_2$	1.16
KCl	0.695
$NaHCO_3$	0.201
KBr	0.101
H_3BO_3	0.027
$SrCl_2$	0.025
NaF	0.003
TDS	42.967

2.4.2 Fouling performance evaluation

The fouling performance evaluations were performed for conforming enhancing anti-fouling efficiency of modified membranes during 24 hours for 2 times after 30 hours compaction step and 1 hour cleaning step with same feed tank condition of compaction step. The cleaning step was conducted with the 4 L/min and no applied pressure. To be precise, put the stock foulant solution immediately after 1 hour cleaning step into the feed tank. In this study, the anti-fouling efficiency of pure and the MPC modified SWRO membranes were evaluated with two model foulants, 30 ppm sodium alginate as polysaccharide foulant and 10 ppm Bovine serum albumin as protein foulant for each set performance test. Also, the flux recovery (FR) test was conducted to evaluate the cleaning efficiency of the membranes after 24 hours 1st fouling performance evaluation. The flux recovery was calculated using the following equations, and the permeate water flux was measured during fouling performance evaluation at the same conditions of the performance test.

$$\text{FR } (\%) = \frac{J_w}{J_i} \; X \; 100 \qquad (3.3)$$

where: J_w : Permeate water flux during fouling performance (L/m^2 h)

J_i : Initial water flux (L/m^2 h)

Chapter 3. Results and discussions

3.1 Attenuated total reflectance-Fourier transform infrared spectroscopy (ATR-FTIR)

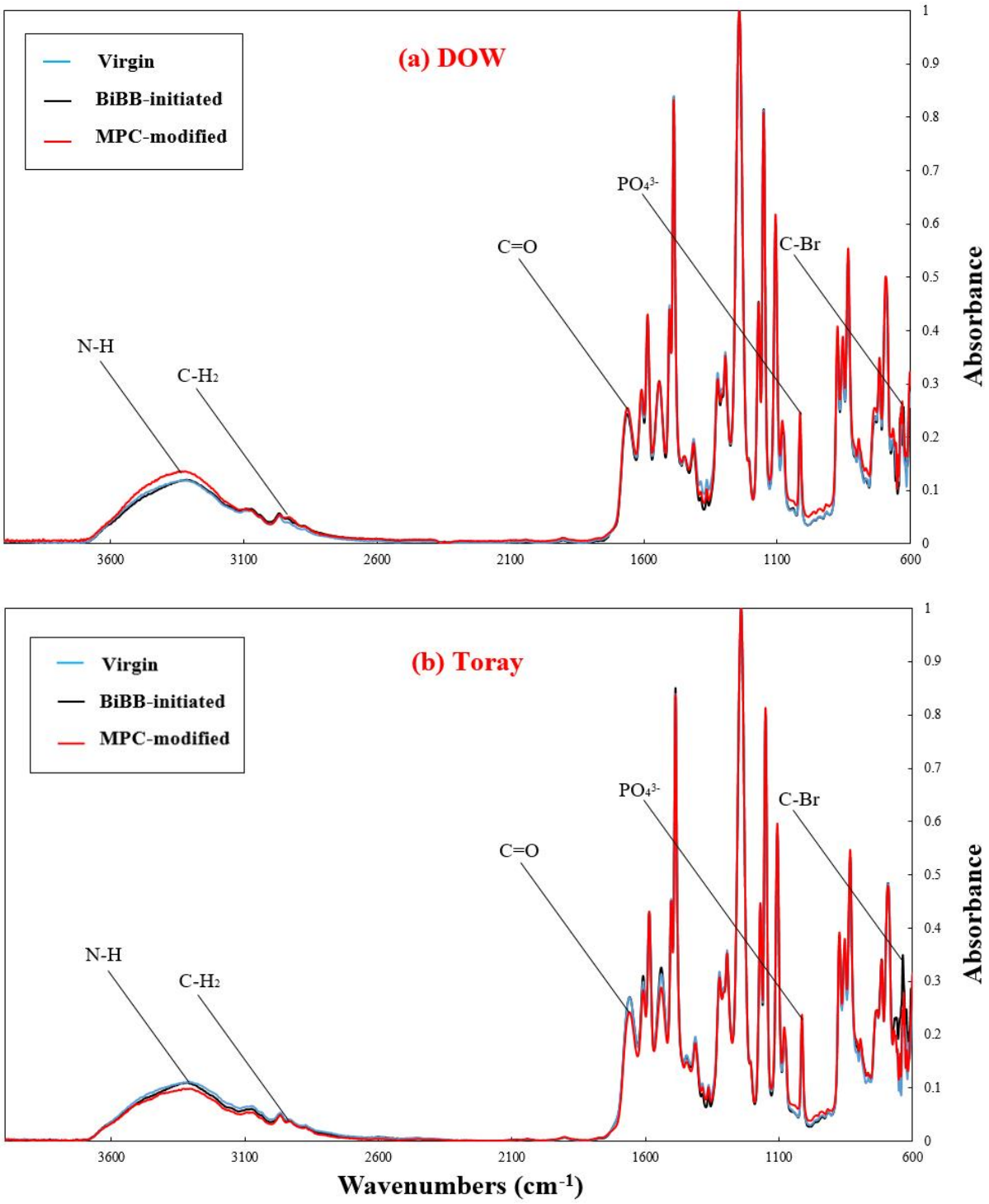

Figure 11. FT-IR spectra of virgin, BIBB-initiated, MPC-modified (a) DOW and (b) Toray membranes

The ATR-FTIR spectra was conducted to identify the functional groups of membrane surface. As shown in above Figure 5. spectra of (a) DOW and (b) Toray membranes FTIR spectra combined with virgin, after BIBB-initiated and MPC-modified reaction for each company membranes from 600 cm^{-1} to 4000 cm^{-1} wavenumbers that can be investigated PA surface active layer and PSf support layer spectra. Furthermore, representative BIBB chemical functional groups C−Br alkyl halides stretching and target zwitterionic chemical MPC chemical functional groups $-POCH_2^-$ phosphate stretching, $N^+(CH_3)_3(CH_2)$ quaternary ammonium ion and C=O carbonyl stretching cab be investigated this spectra range wavenumber. To analyze the two spectra (a), (b) in Figure 5, at 1589 and 1491 cm^{-1} wavenumbers were investigated PSf support layer aromatic carbon C=O peaks, at 2933 and 3298 cm^{-1} wavenumbers were investigated PA surface active layer for each wavenumber assigned C−H_2 and N−H amide functional groups. Also can be investigated BIBB-initiated carbon C−Br at 615 cm^{-1} wavenumbers, at 1080 cm^{-1}, 1240 cm^{-1} wavenumbers assigned $-POCH_2^-$ phosphate stretching and through 970 cm^{-1} wavenumber, $N^+(CH_3)_3(CH_2)$ quaternary ammonium ion, can be detected of target zwitterionic chemical MPC on the membranes surface. Each chemical functional groups of virgin, BIBB-initiated and MPC-modified membranes were identifiable, however, no noticeably increased absorbance were investigated. Therefore, further analysis such as XPS, SEMS and Water contact angle were conducted for more detailed and visible confirmation of surface modification.

3.2 X-ray photoelectron spectra (XPS)

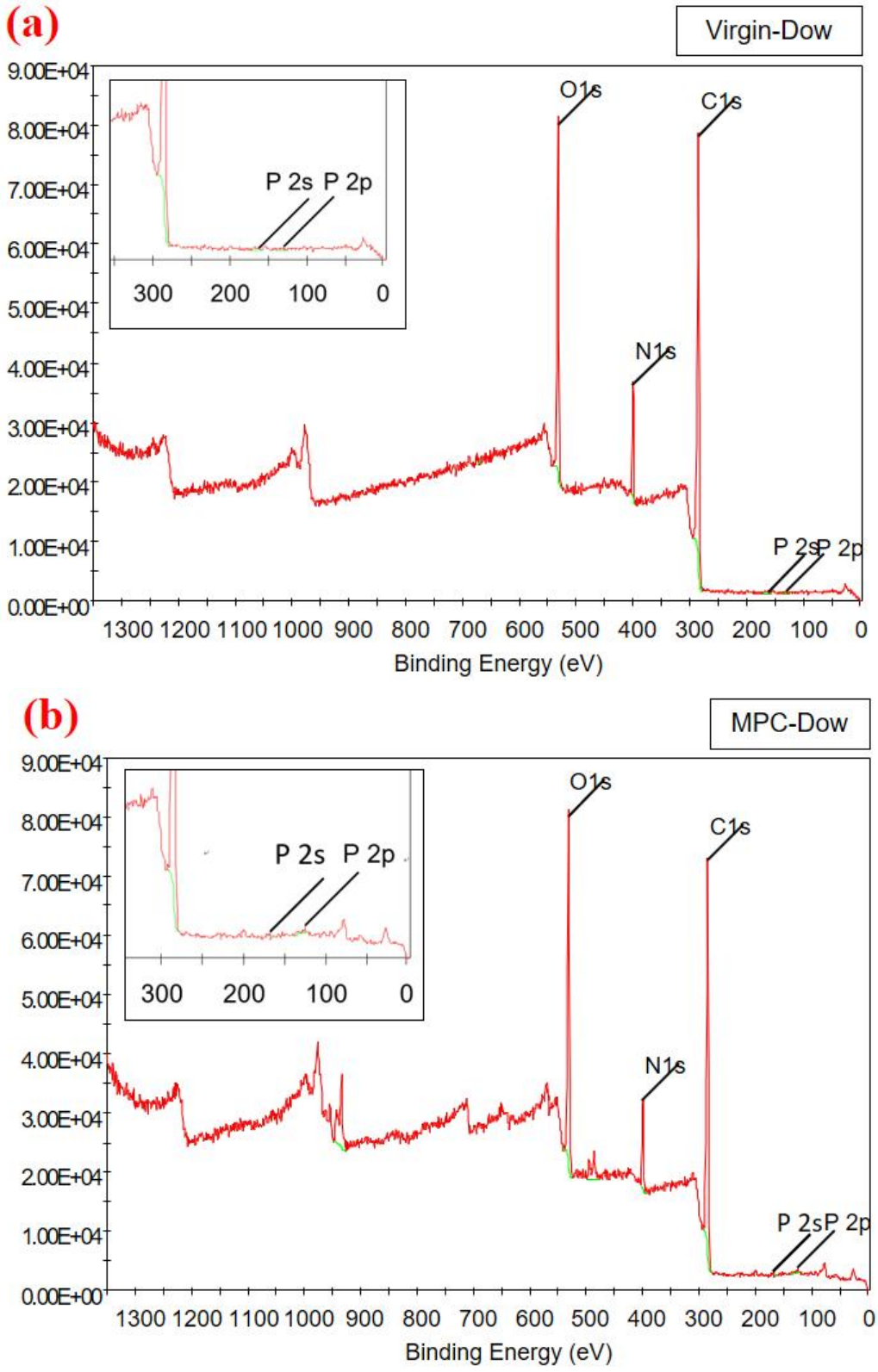

Figure 12. XPS wide scan spectra of (a) Virgin and (b) MPC-modified DOW membrane with the enlarged P peak

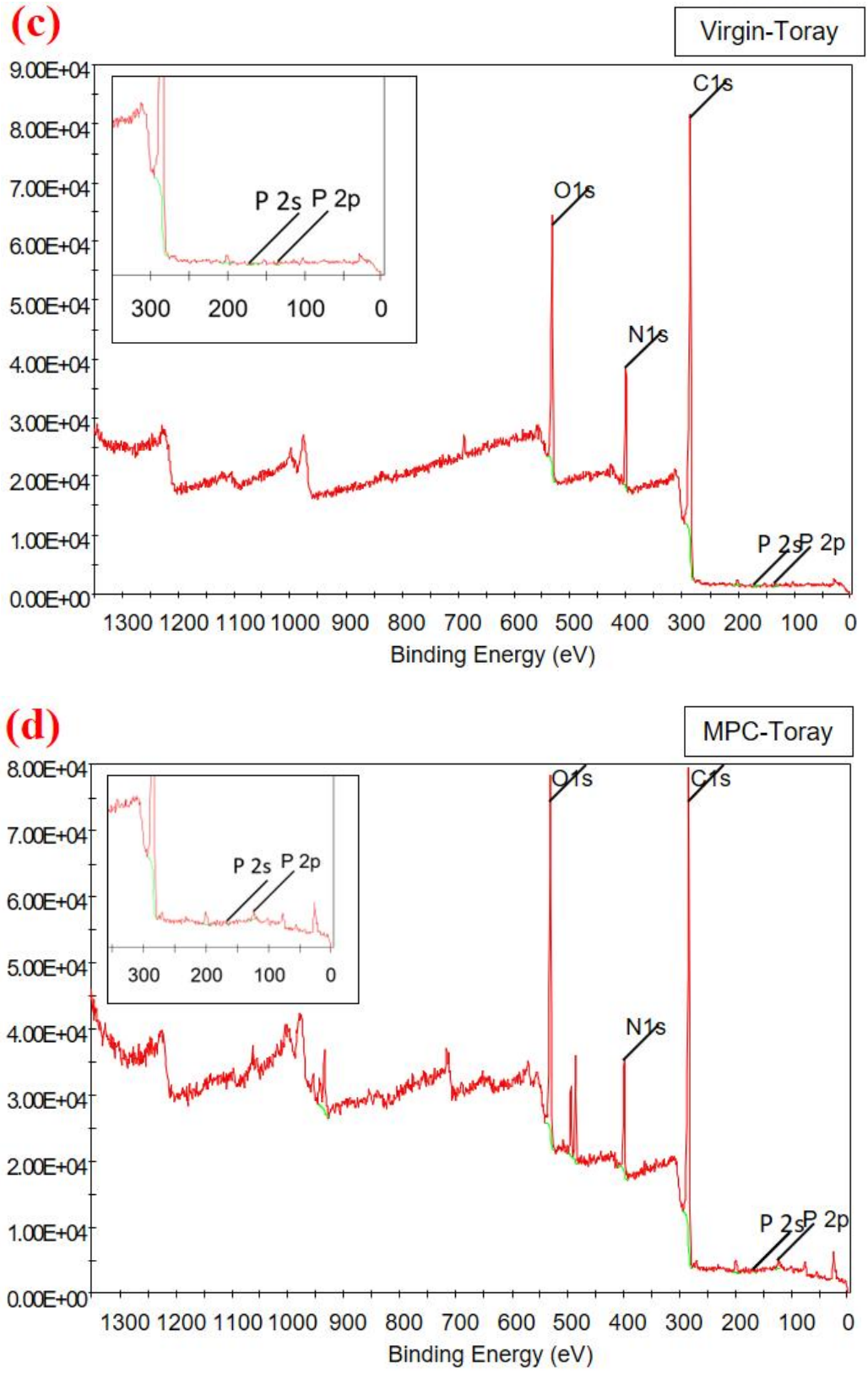

Figure 7. XPS wide scan spectra of (a) Virgin and (b) MPC-modified Toray membrane with the enlarged P peak

As shown in Figure 6,7, XPS wide scan spectra of each company's virgin and MPC-modified membranes with the enlarged P atoms peak regard as atomic concentration (C %) change of carbon (C), nitrogen(N), oxygen (O) and phosphorus (P) in the range of 0 to 1400 eV. First, it can be seen that the phosphorus group P2s and P2p peaks were detected at 172.0, 133.0 eV each, and the intensity of the p part increased as the MPC was modified on membrane surface. Also, the N1s protonated nitrogen atom in ammonium functional group peak was detected at 404.0 eV and increased as the MPC was modified seems like phosphorus group. And the C1s was detected at 286.4 eV that according to ester bond in the methacrylate group at the MPC. Comparing the data in the two tables (Table 2,3.) below, it can see that the ratio of O and P parts increases while MPC is modified, however the ratio of C and N parts decreases. This is because that the proportion of P and O occupies a larger proportion in the MPC molecule relative to C and N as MPC is modified.

Table 2. Comparative atomic concentration ratio (C, N, O, and P) of Virgin and MPC modified DOW membrane.

Membrane	**Carbon (Atomic C %)**	**Nitrogen (Atomic C %)**	**Oxygen (Atomic C %)**	**Phosphorus (Atomic C %)**
Virgin-DOW	71.37	8.31	20.22	0.1
MPC-DOW	67.01	7.54	24.03	1.41

Table 3. Comparative atomic concentration ratio (C, N, O and P) of Virgin and MPC modified Toray membrane.

Membrane	**Carbon (Atomic C %)**	**Nitrogen (Atomic C %)**	**Oxygen (Atomic C %)**	**Phosphorus (Atomic C %)**
Virgin-Toray	74.62	9.09	16.29	0
MPC-Toray	69.01	8.42	20.77	1.80

3.3 Scanning electron microscopy (SEM)

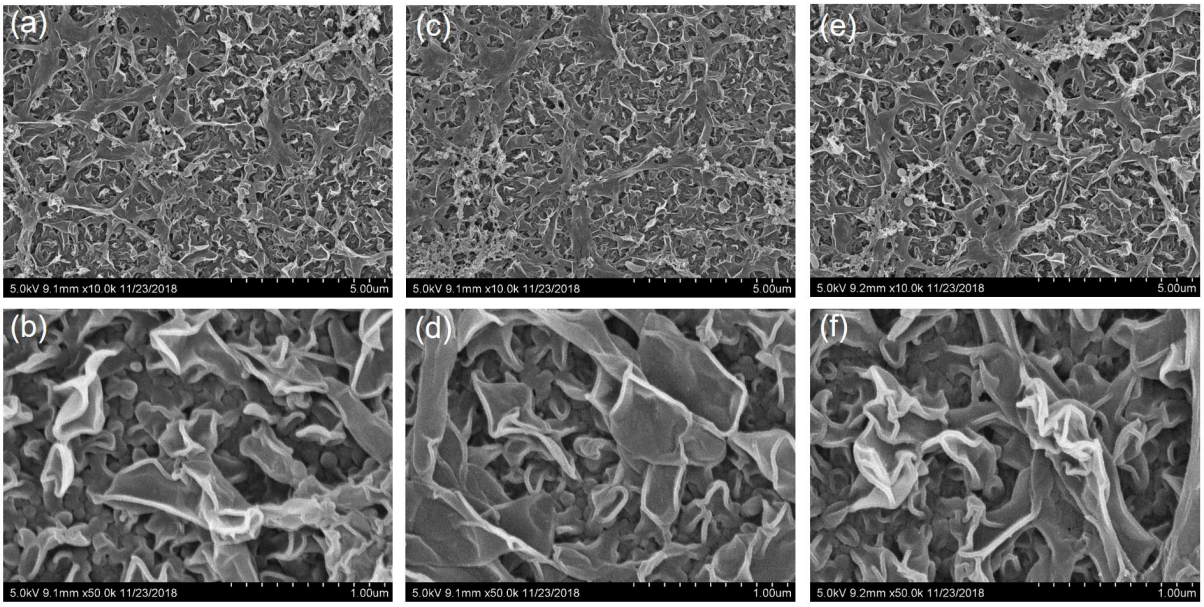

Figure 8. Surface morphology images of virgin, BIBB initiated, MPC modified DOW membrane. (a), (b) virgin membrane, (c), (d) BIBB initiated membrane and (e), (f) MPC modified membrane each.

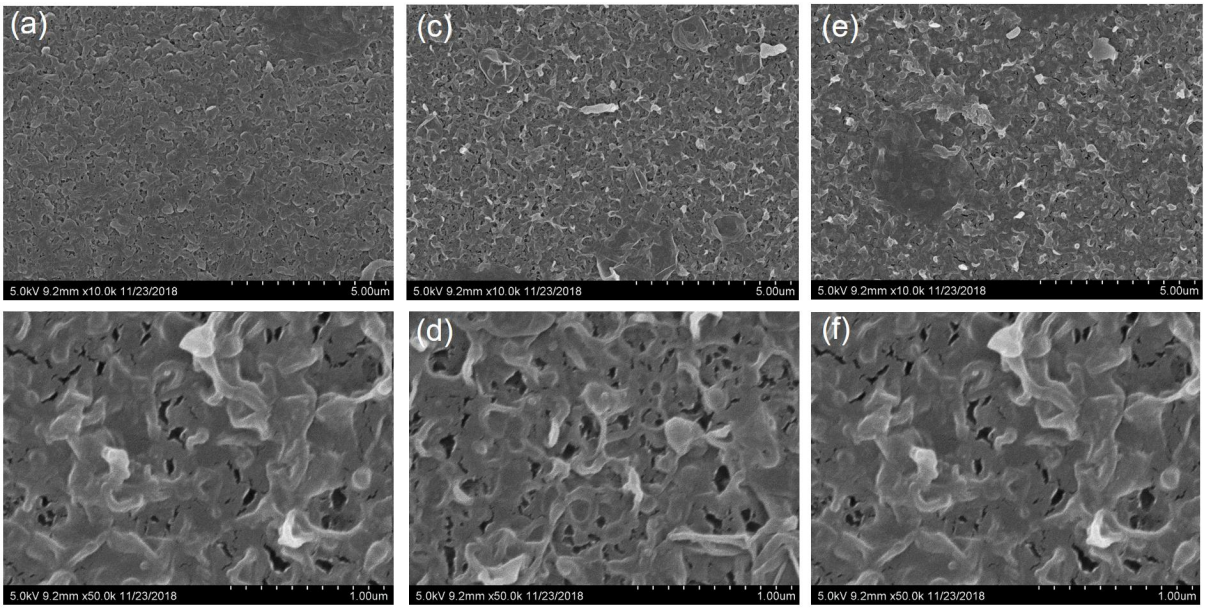

Figure 9. Surface morphology images of virgin, BIBB initiated, MPC modified Toray membrane. (a), (b) virgin membrane, (c), (d) BIBB initiated membrane and (e), (f) MPC modified membrane each.

As results from Figure 8, 9, the surface morphology images of virgin, BIBB initiated and MPC modified membranes of each companies by SEM. In Figure 7, all SEM images of DOW membrane surface morphology has valley and ridge structure comparing with Figure 8 Toray membrane SEM images that has smooth and soft. Also, as surface modification steps were progressed (from left to right images), can confirm that little bit cells adhered and spread of MPC on the membrane.

3.4 Water contact angle

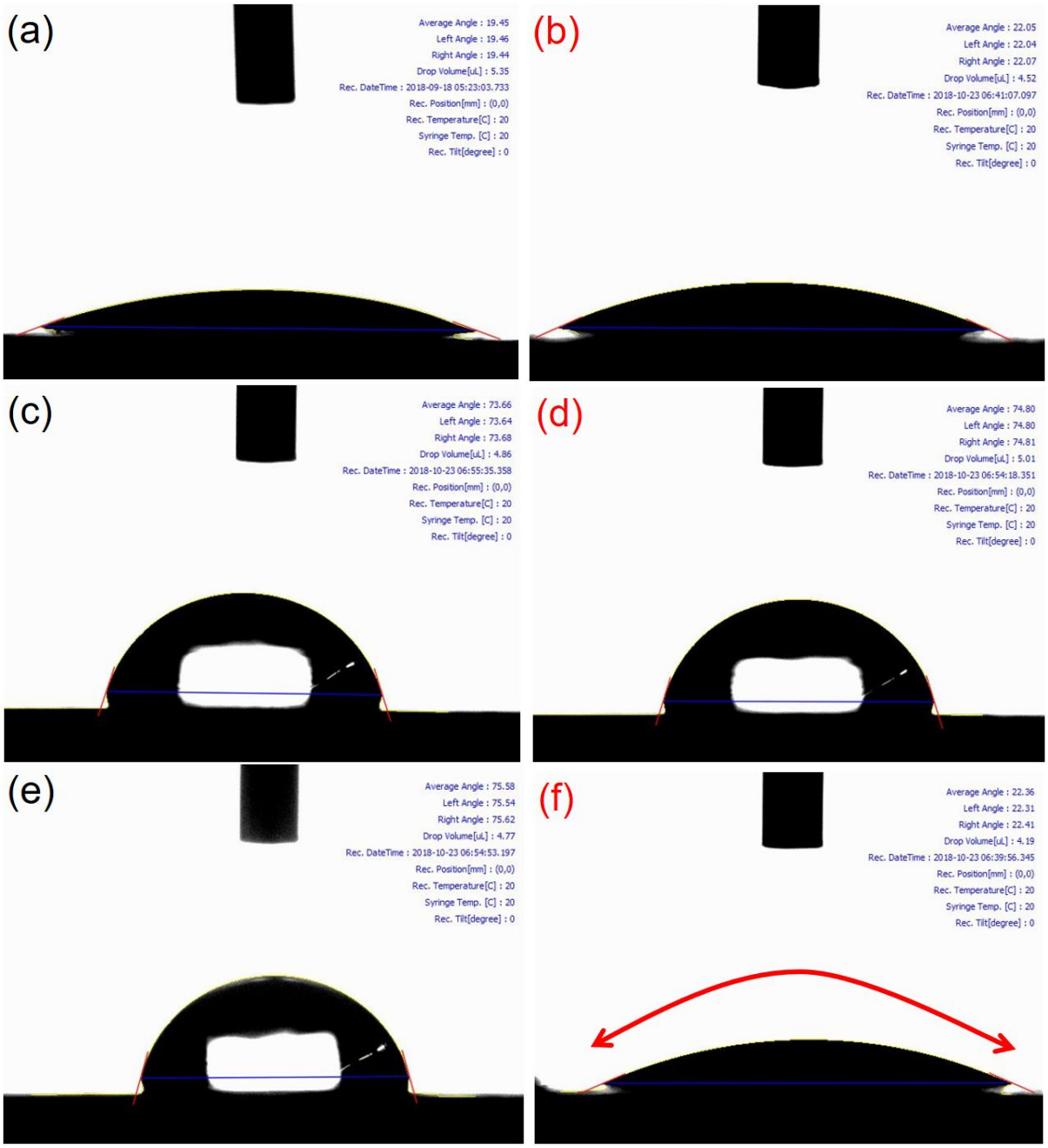

Figure 10. Surface contact angle images of virgin, BIBB initiated and MPC modified DOW membranes. (a), (c), (e) are drops of DI water contact angle of virgin, BIBB initiated and MPC modified respectively. (b), (d), (f) are drops of artificial seawater contact angle of virgin, BIBB initiated and MPC modified respectively.

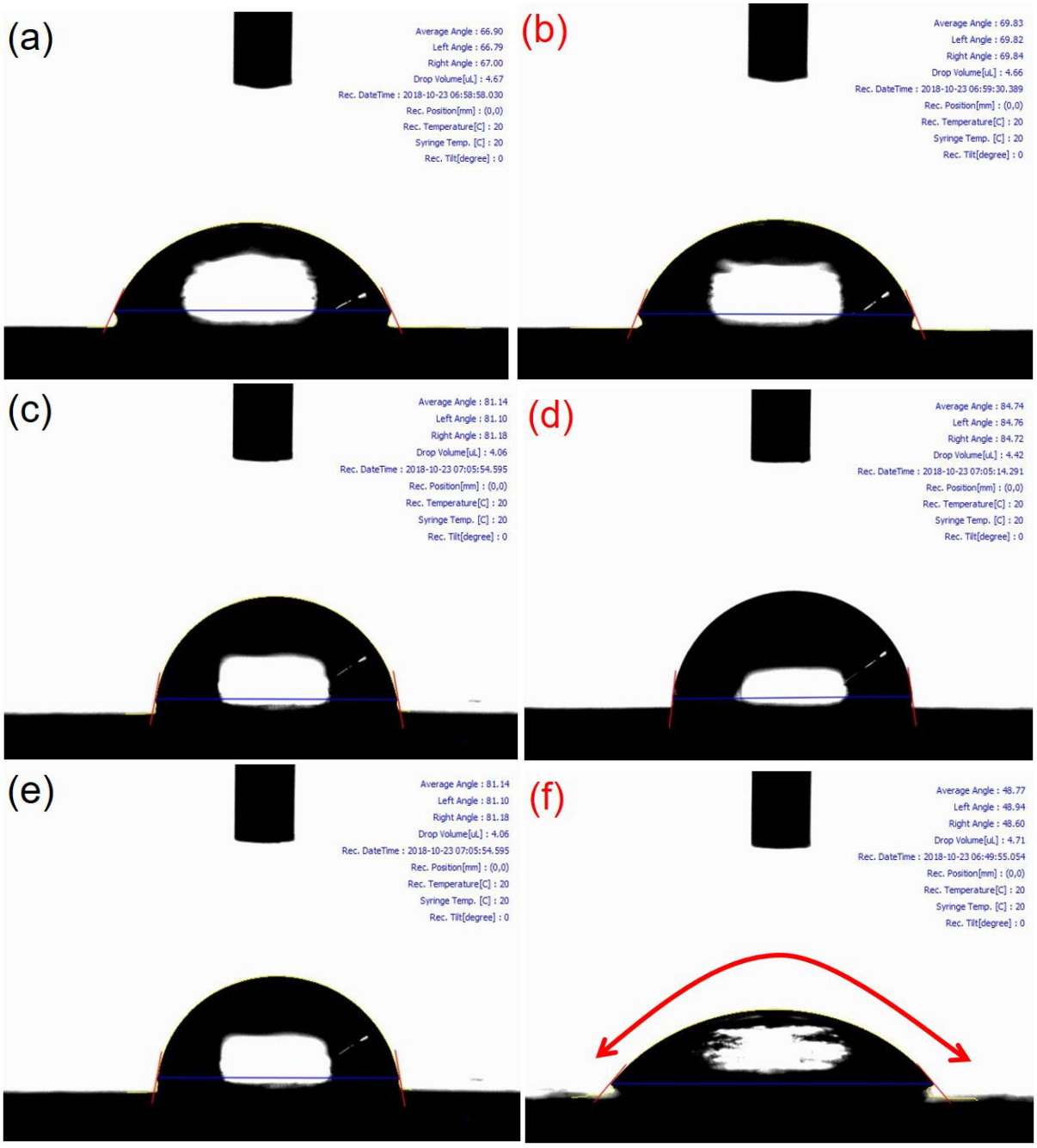

Figure 11. Surface contact angle of virgin, BIBB initiated and MPC modified Toray membranes. (a), (c), (e) are drops of DI water contact angle of virgin, BIBB initiated and MPC modified respectively. (b), (d), (f) are drops of artificial seawater contact angle of virgin, BIBB initiated and MPC modified respectively.

From results Figure 9, 10, the surface contact angle results of virgin, BIBB initiated and MPC modified membranes results as DOW and Toray, respectively. Contact angle was measured with two different drop solution, one is DI water and another is artificial seawater solution as same as feed tank condition solution. So, (a), (c), (e) images were results with DI water and (b), (d), (f) images were results with artificial seawater as two figures. For more detailed results, graph was displayed in Figure 11, 12, first of all, both graph results show the same tendency. That is because the difference of virgin membrane contact angle degree, the Dow membrane treated hydrophilic coating treatment has been applied since the production but didn't treat on the Toray membrane. When BIBB initiated step were conducted, the contact angle of both DI water and artificial seawater was increasing due to the hydrophobic nature of the BIBB attached to the surface of virgin membranes. Also, when dropped the DI water on the MPC modified membranes, the contact angle was almost same or little bit increased. However, when dropped the artificial seawater solution on the MPC modified membranes, the contact angle was sharply decreased to the same level of virgin membrane. This tendency was detected on both DOW and Toray membranes. This principle occurs when in case of zwitterionic chemical like MPC had both negatively charged and positively charged groups in one molecular in this study. These oppositely charged groups exhibit strong interactions between them and expose hydrophobic hydrocarbon radicals to the surface. "Salting-in effect" is the electrostatic properties of each group were shown by the addition of artificial seawater and resulted from the expansion of the volume transition coating layer.

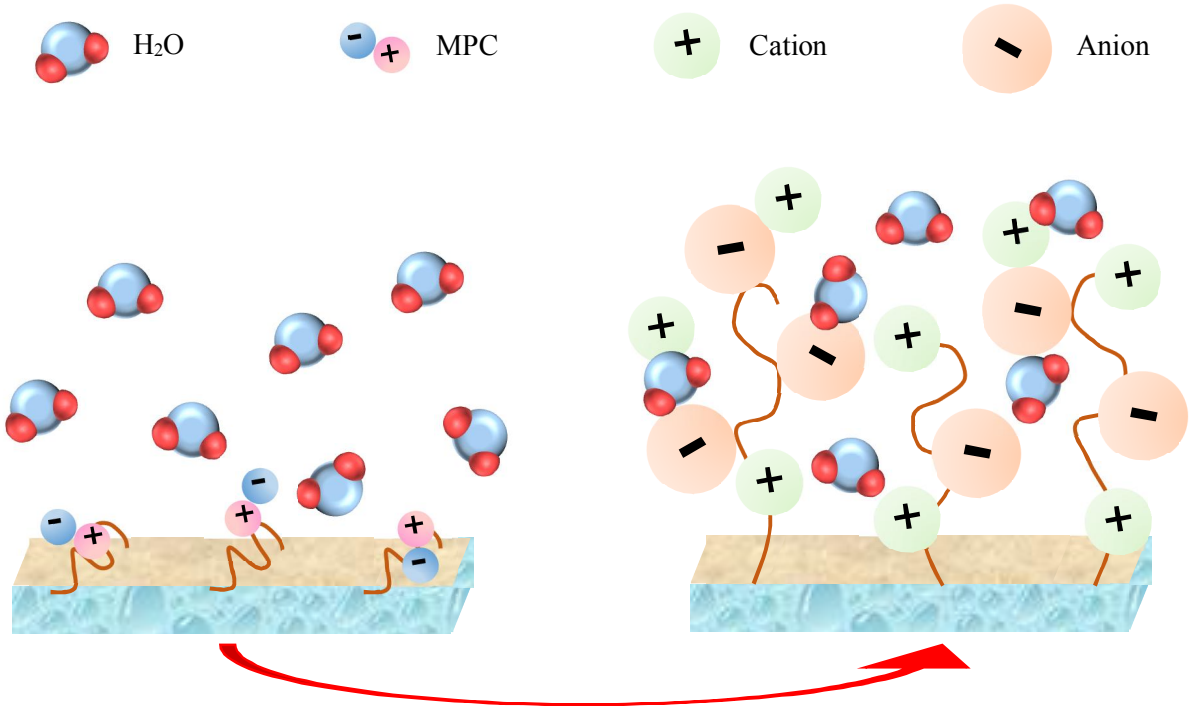

Figure 12. Illustration of "salting-in effect" on MPC-modified membrane in the artificial seawater

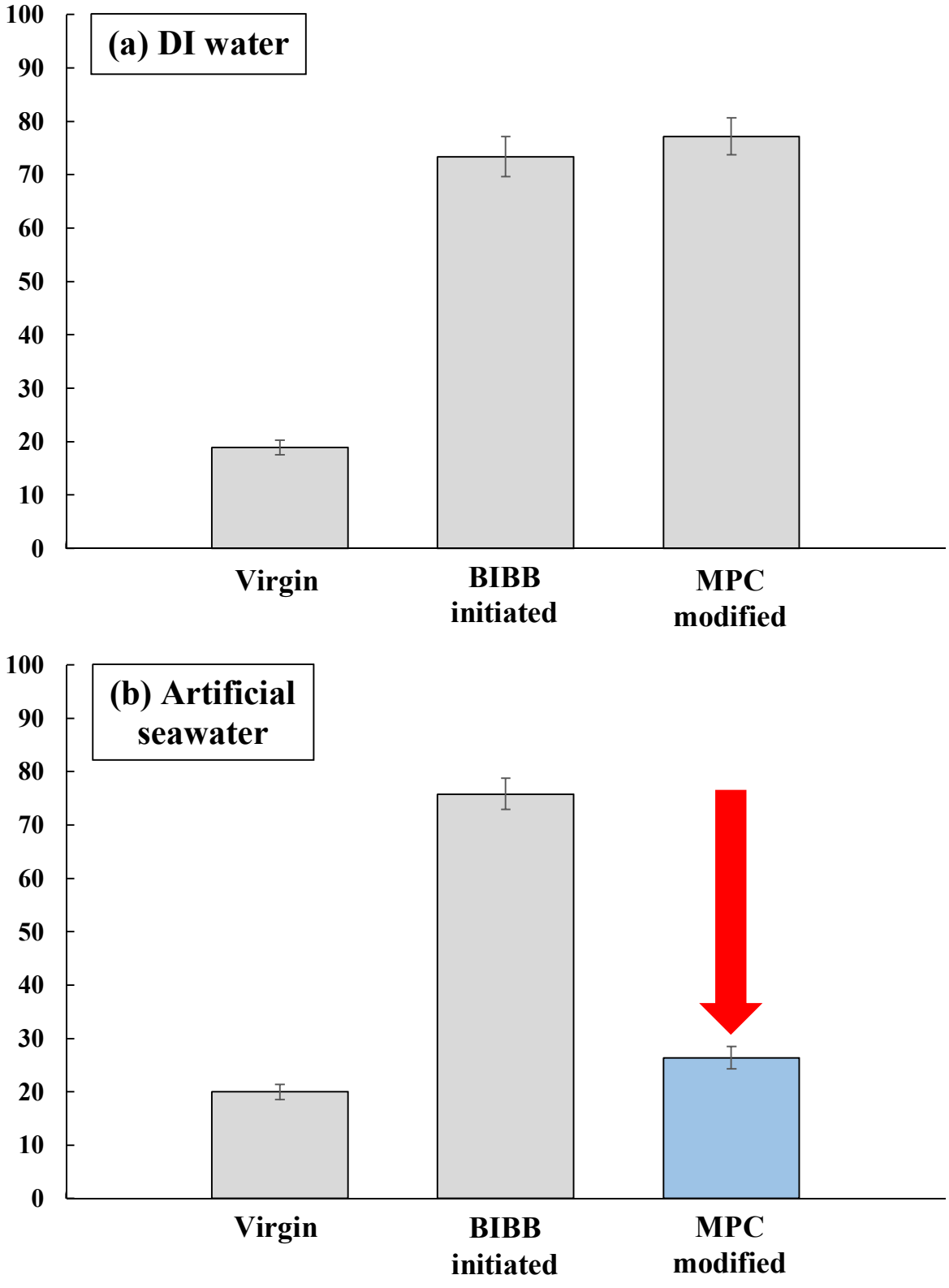

Figure 13. Drop contact angle of (a) DI water, (b) artificial seawater on DOW membranes.

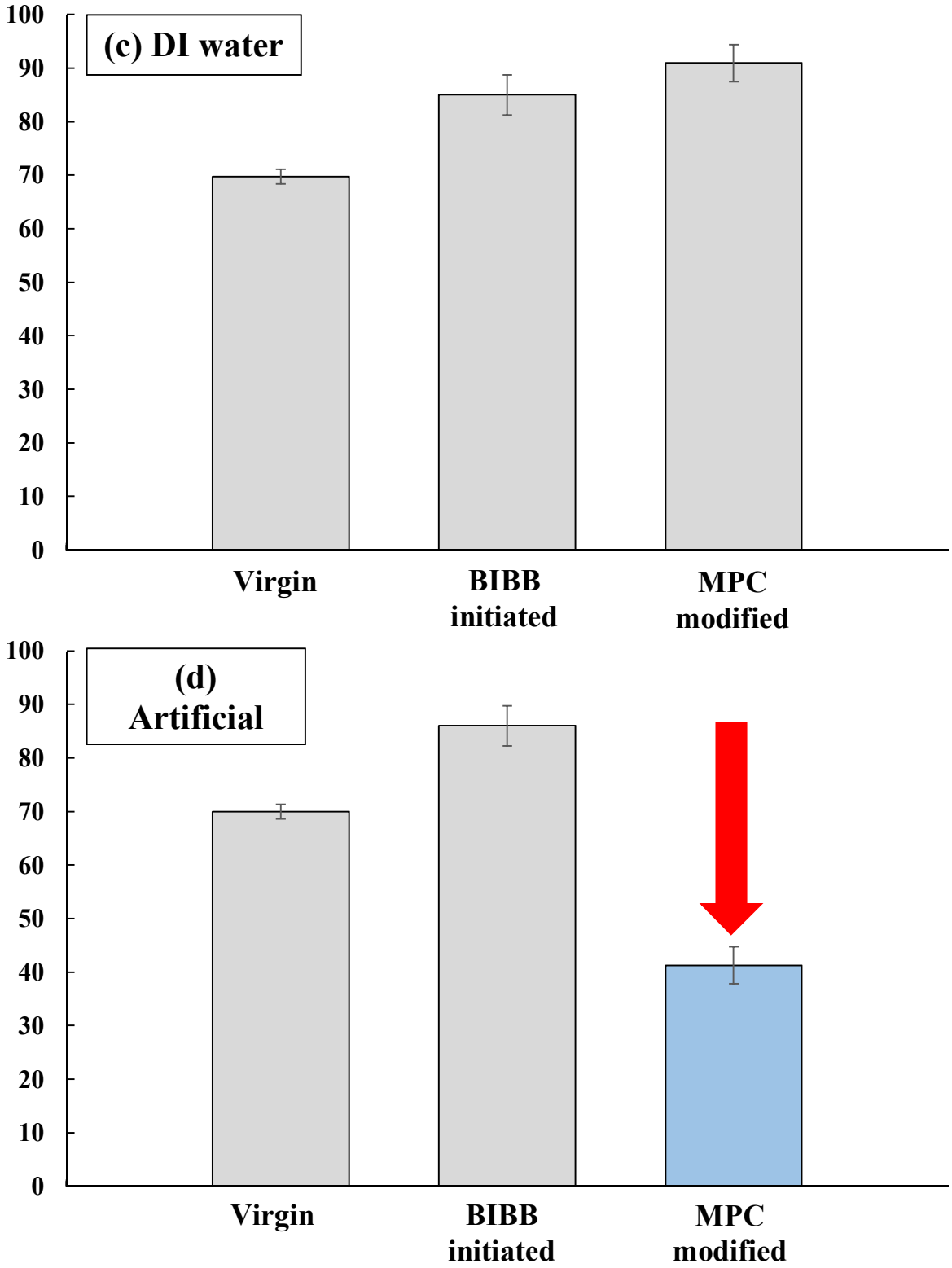

Figure 14. Drop contact angle of (a) DI water, (b) artificial seawater on Toray membranes.

3.5 Membrane performance evaluation

3.5.1 Fouling performance test: Compaction step

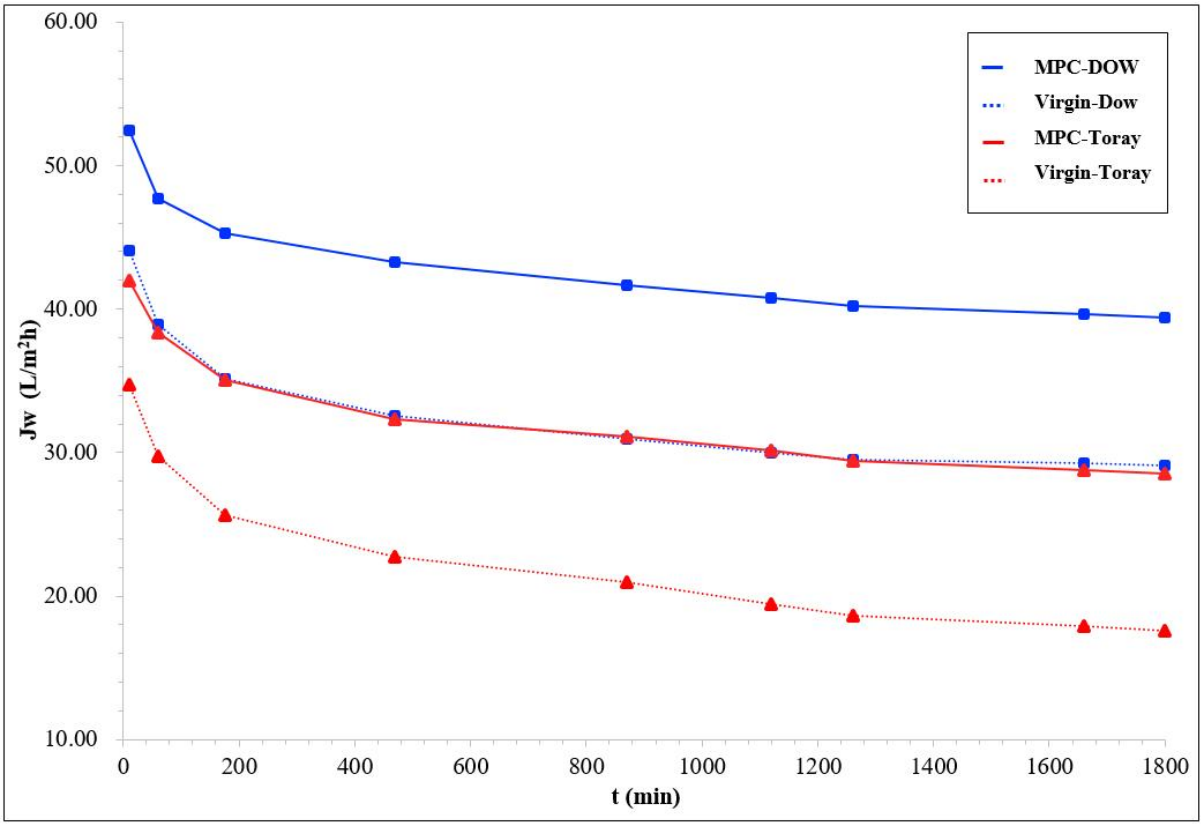

Figure 15. Flux decline tendency of virgin and MPC modified SWRO membranes during 30 hours membrane compaction step in artificial seawater feed tank condition for with sodium alginate test

The fouling performance test was evaluated with two model foulants sodium alginate and bovine serum albumin. So whole test was conducted total of two tests. As shown in figure 14, 16, the initial water permeate fluxes of the virgin membranes for DOW and Toray were 44.1 L/m^{2}h and 34.7 L/m^{2}h (in figure 14), 45.4 L/m^{2}h and 32.6 L/m^{2}h (in figure 16) respectively (Dotted line). Then, initial water permeate flux of the MPC modified membranes for DOW and Toray were 52.5 L/m^{2}h and 42.0 L/m^{2}h (in figure 14), 52.3 L/m^{2}h and 41.3 L/m^{2}h (in figure 16) respectively (Solid line). Therefore, when the MPC modified on the membrane surface, both company membranes initial water permeate flux were increased. Comparing the tendency of virgin and MPC modified membrane respectively, the hydrophilicity of the membrane surface was increased as entire evaluation time. Also, through the figure 15, salt rejection data during 30 hours membrane compaction step, shows the stable tendency rejection data remained steady at levels between 99.2 and 99.25 degree. In figure 17 shows also stable tendency

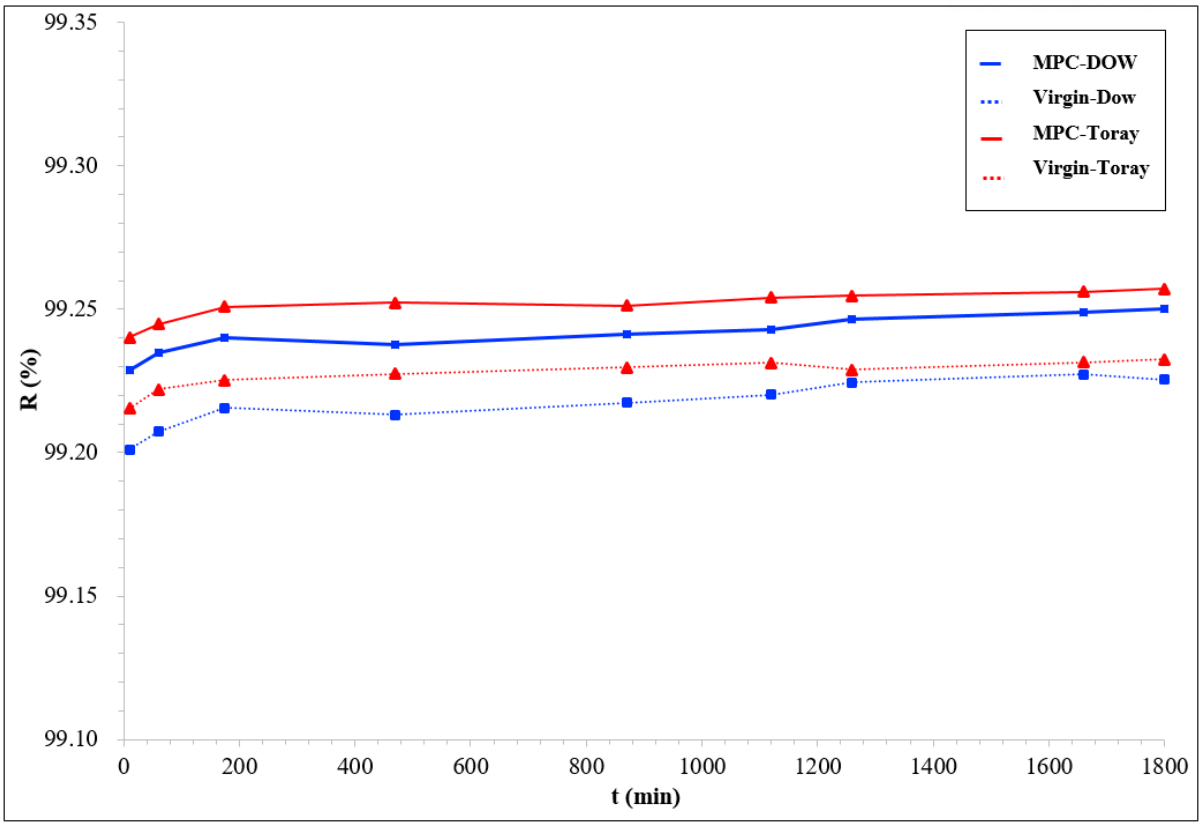

Figure 16. R (%), salts rejection, data of virgin and MPC modified SWRO membranes during 30 hours membrane compaction step in artificial seawater feed tank condition for with sodium alginate test.

rejection data remained steady at levels between 99.1 and 99.22 degree. These results mean that the surface modification of SWRO membranes with zwitterinoic chemical MPC was approximately successful with no defect on the membrane surface.

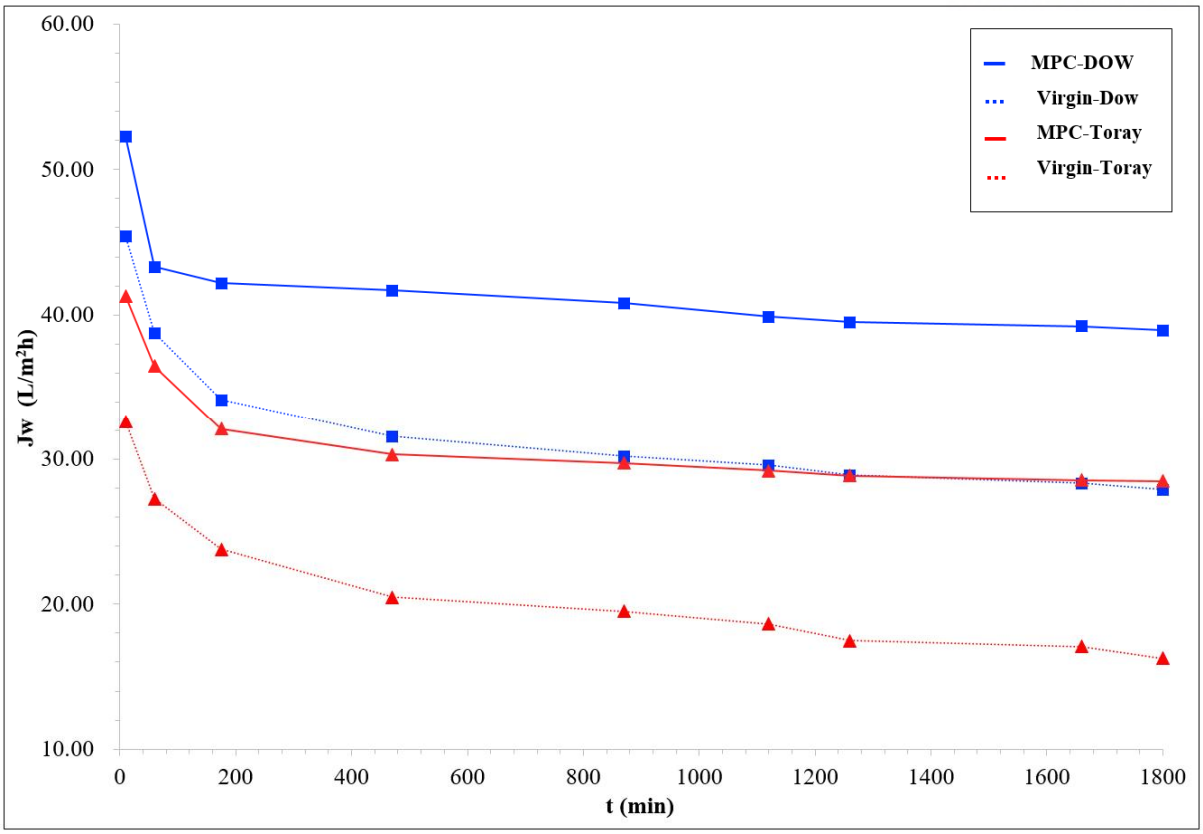

Figure 17. Flux decline tendency of virgin and MPC modified SWRO membranes during 30 hours membrane compaction step in artificial seawater feed tank condition for with BSA test

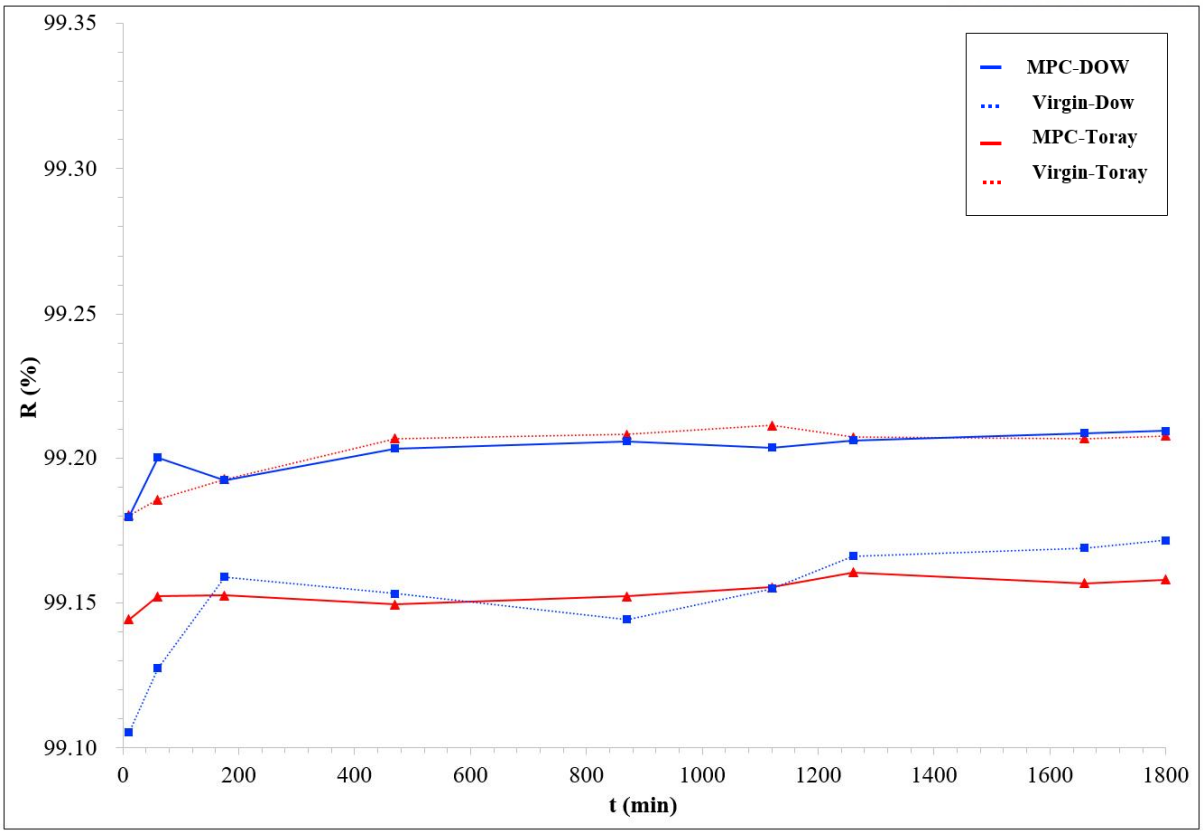

Figure 18. R (%), salts rejection, data of virgin and MPC modified SWRO membranes during 30 hours membrane compaction step in artificial seawater feed tank condition for with BSA test.

3.5.2 Fouling performance test: 2 sets fouling test

As shown in figure 18, 20, then after finishing the 30 hours compaction step, immediately put the model foulant 30 ppm sodium alginate solution into 30 L feed tank and begin the two set of anti-fouling performance test during 24 hours (total 24 hours). As soon as adding 30 ppm sodium alginate and 10 ppm bovine albumin serum solution, it can see that the flux tendency was drastically decreased because adsorption of sodium alginate on to the surface that they block the pores. Therefore, the flux decline tendency after beginning the fouling test was lower than during compaction step's tendency, as time went on, the lowest flux was also lower when finally stabilized. After the 1st set of fouling performance test, wash the membrane with no applied pressure and put in new model foulant solution with new artificial seawater feed solution prepared it beforehand. Then, the flux decline tendency also decreased in 2nd test but lower than the 1st test, because some of the accumulated foulants that were not completely removed. However, when the flux decline stabilized over time, the lowest flux of 2nd test was lower than the 1st set of flux. Besides, comparing the finally reduced flux of virgin and MPC modified membrane as both DOW and Toray company respectively, the MPC modified membrane's

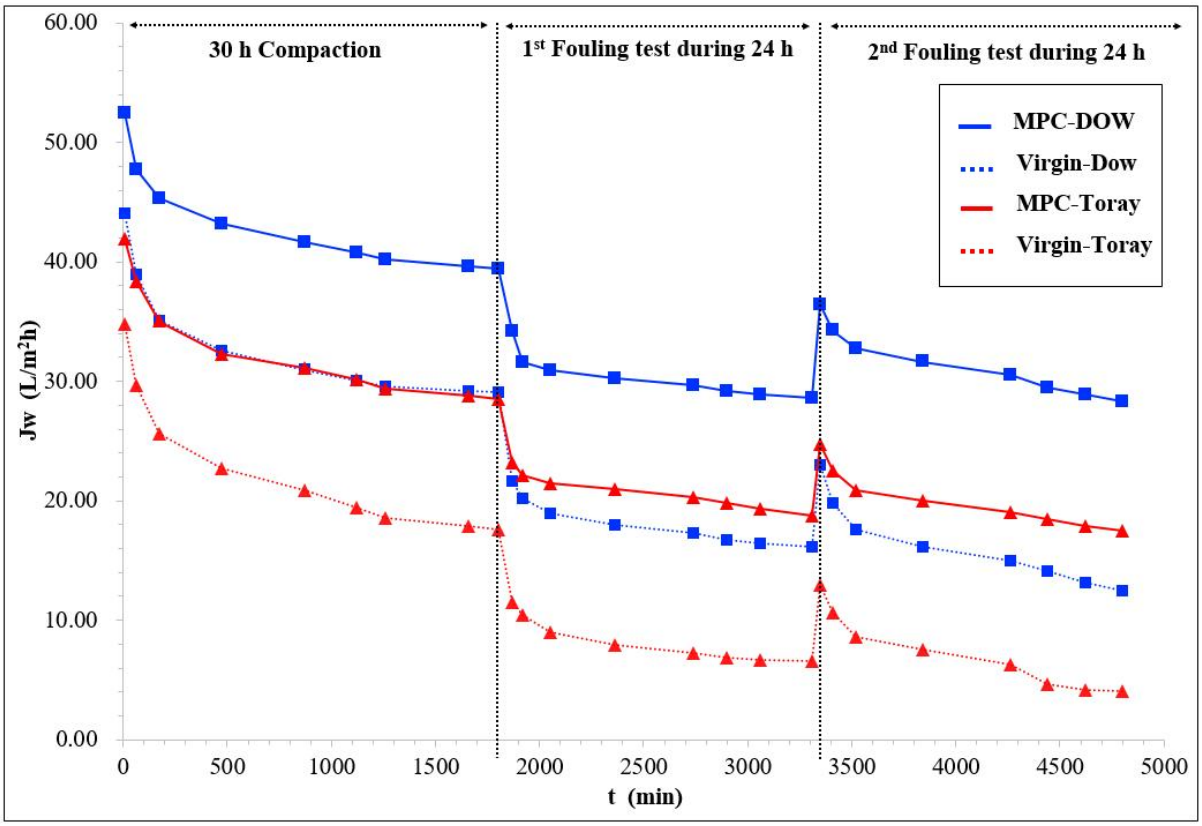

Figure 19. Flux decline tendency of virgin and MPC modified membrane during total fouling performance test with 30 ppm sodium alginate in artificial SW feed tank conditions

decreased level of flux than the virgin membrane. Likewise, it shows that MPC increasing high hydrophilicity of virgin membrane more than before. Also, through the figure 19, 21, R (%) data during fouling performance test, unlike the flux tendency, the rejection was increased when the immediately put the model foulant 30 ppm sodium alginate and 10 ppm bovine albumin serum solution into 30 L feed tank respectively. During the 1st set of anti-fouling test, the rejection tendency was quickly stabilized than flux tendency. When the 2nd test beginning, unlike the flux tendency, there is no big tendency change between 1st and 2nd set of anti-fouling test. The flux recovery (FR, %) efficiency of the membranes based on normalized permeate water flux, during anti-fouling test was measured and shown in figure 22, 23 and it was calculated at finished 1st anti-fouling performance test. The initial water flux was measured at last sampling point during compaction steps, then normalized flux was measured based on this initial permeate water flux. First, in case of the test with 30 ppm sodium alginate in figure 22, the FR of two virgin membranes DOW and Toray is 79.22 % and 73.81 % respectively. Then the FR of two MPC modified membranes is 92.51 % and 86.79 %, that increased 13.29 % and 12.98 % degree. Likewise, in case of the test with 10 ppm bovine albumin serum as a model foulant in figure 23, the FR of two virgin membranes DOW and Toray is 81.33 % and 75.83 %

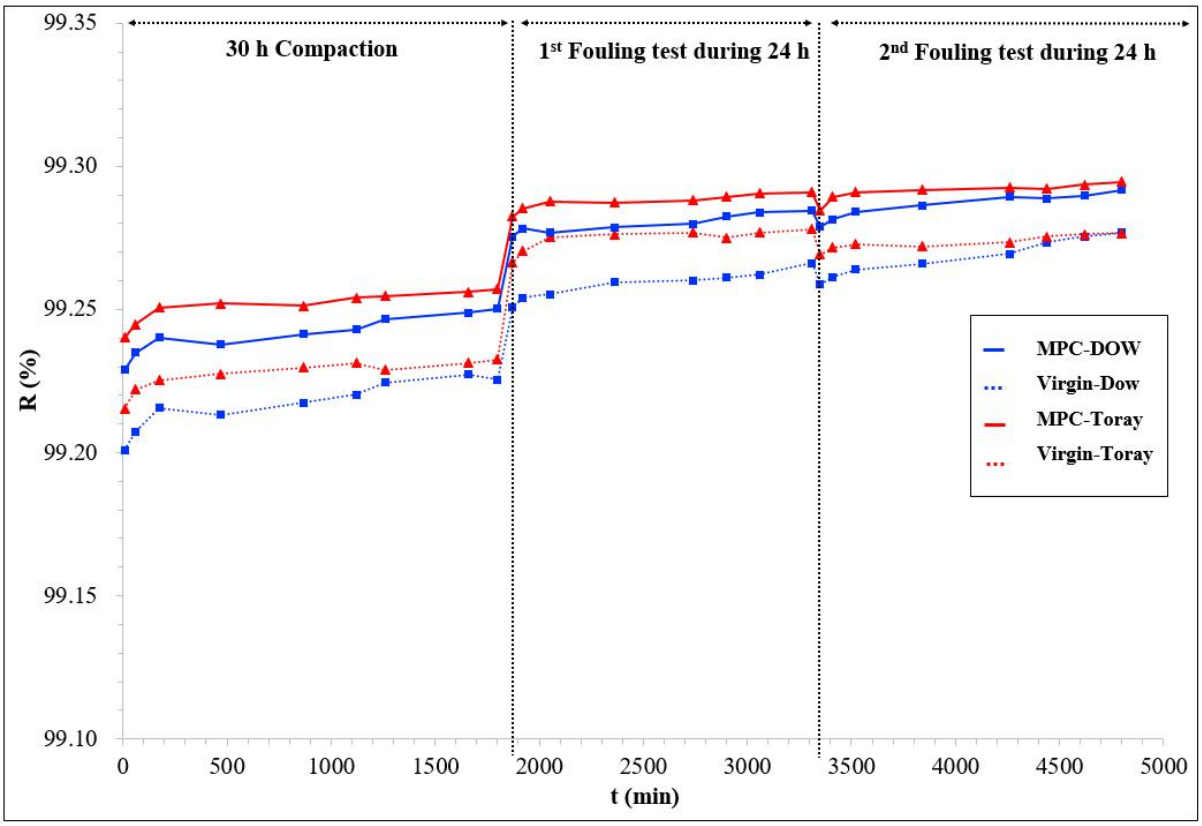

Figure 20. R (%), salts rejection, data of virgin and MPC modified SWRO membranes during total fouling performance test with 30 ppm sodium alginate in artificial SW conditions

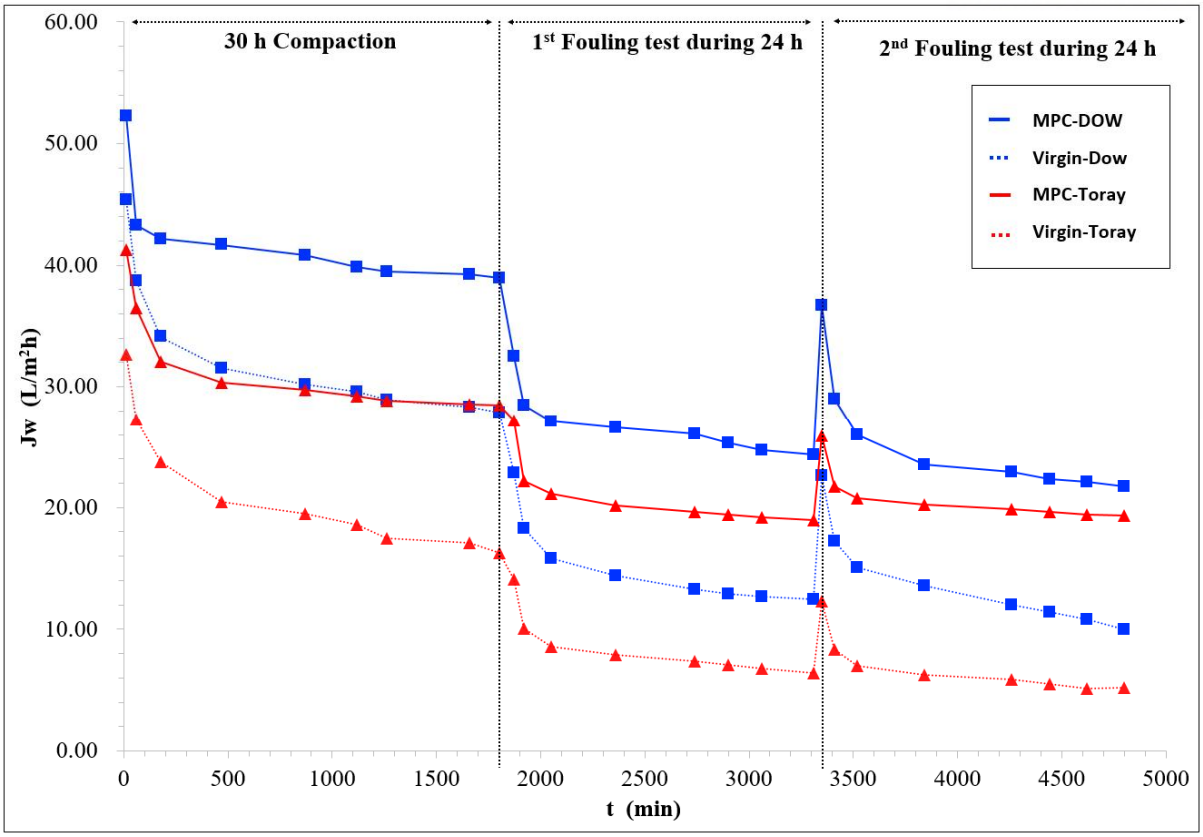

Figure 21. Flux decline tendency of virgin and MPC modified SWRO membrane during total fouling performance test with 10 ppm bovine albumin serum in artificial SW feed tank conditions

respectively. Then the FR of two MPC modified membranes is 94.21 % and 91.13 %, that increased 12.88 % and 15.3 % degree. The stabilized water permeate flux at the last point of 2nd fouling test, the MPC modified membranes flux has higher levels than the virgin membranes. Therefore, can say that when MPC modified membranes increased hydrophilicity of membrane surface, then this effect increases the membrane flux recovery efficiency with enhanced fouling resistance. The target zwitterinoic chemical MPC grafted on the TFC SWRO membrane surface, then this form the hydration layer above coating layer. So, through this hydration layer, water molecules passing vigorously than before. Through this from 30 hours compaction to total time is 24 hours of 2 set anti-fouling performance test shows the potentiality when the zwitterionic chemical grafted on the SWRO membrane surface, the long-term operation is possible that applied to actual process.

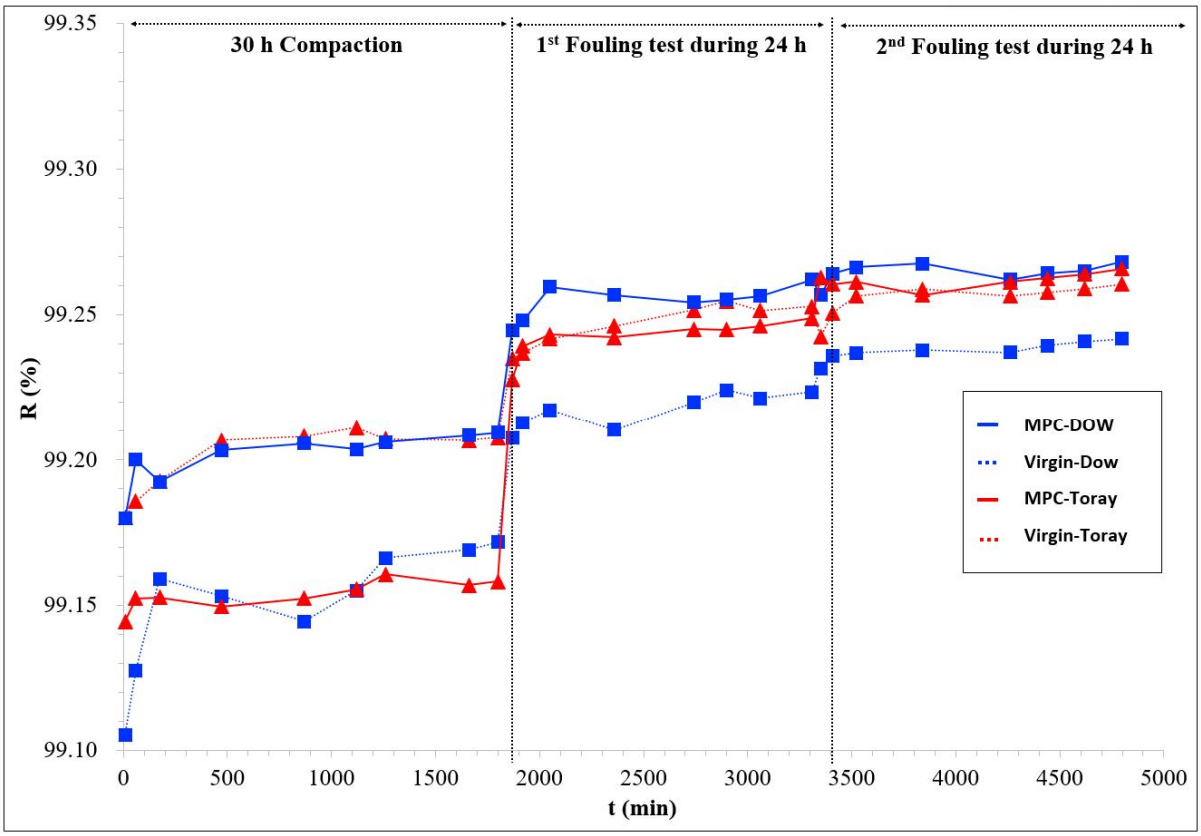

Figure 22 R (%), salts rejection, data of virgin and MPC modified SWRO membranes during total fouling performance test with 10 ppm bovine albumin serum in artificial SW conditions

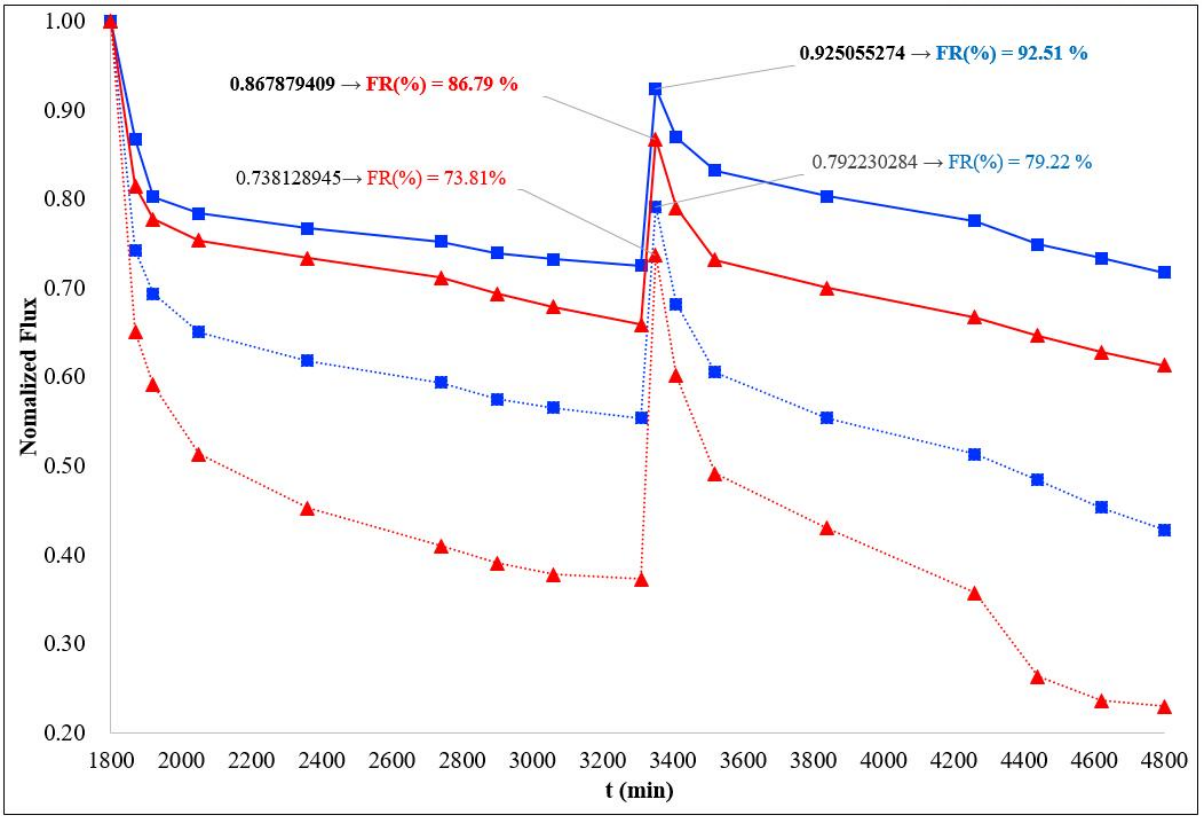

Figure 23. Nomalized flux tendency and FR (%), flux recovery, of virgin and MPC modified SWRO membrane during 1st and 2nd anti-fouling performance test with 30 ppm sodium alginate in artificial SW condition

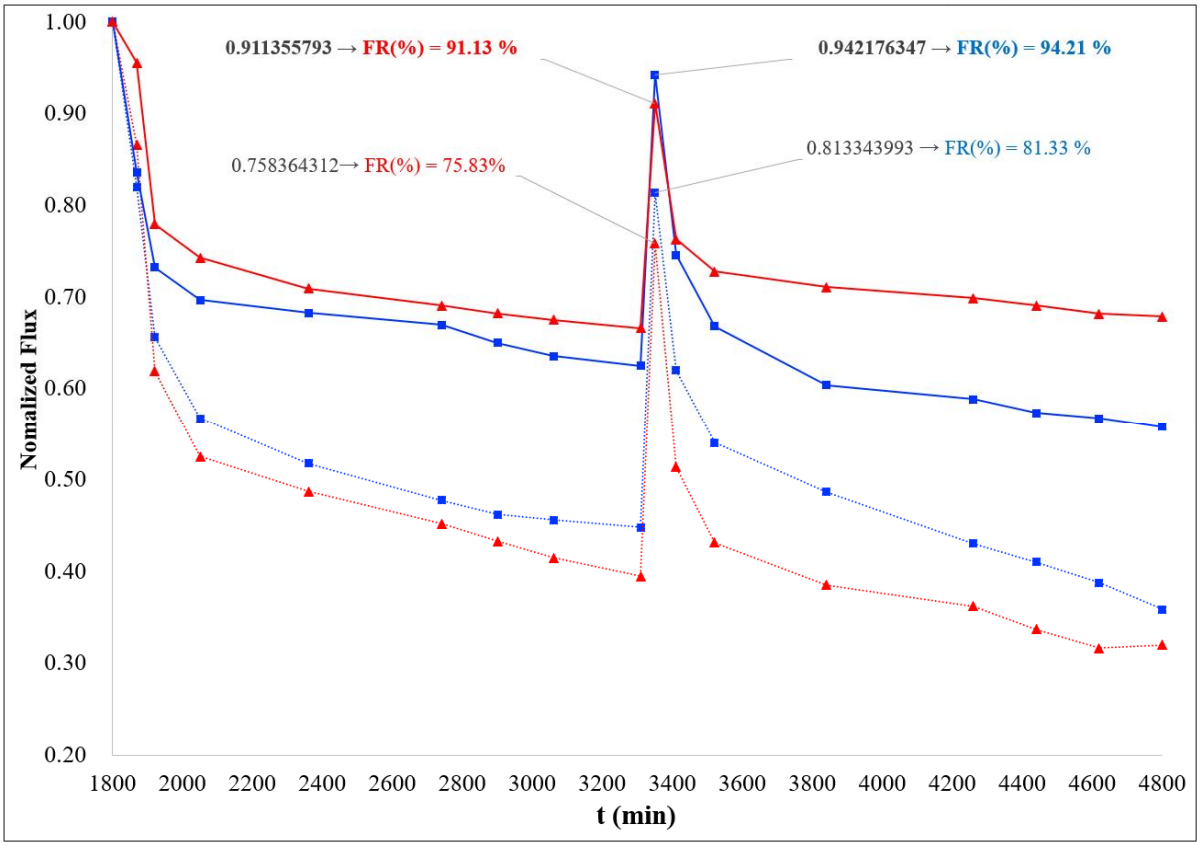

Figure 24. Nomalized flux tendency and FR (%), flux recovery, of virgin and MPC modified SWRO membrane during 1st and 2nd anti-fouling performance test with 10 ppm bovine albumin serum in artificial SW condition

Chapter 4. Conclusions

In this study, conducted the surface modified of commercially available polyamide based TFC SWRO membranes with the target zwitterionic chemical MPC through the surface modification by surface-initiated atom transfer radical polymerization (si-ATRP) for enhancing anti-fouling capability.

Zwitterinoic chemical MPC grafted on the TFC SWRO membrane surface, that was conducted formation of hydration layer above the coating layer. Then through this hydration layer, water molecules passing vigorously than before and increasing the hydrophilicity of the MPC modified membrane surface. To confirm the successful modification, several analytical methods were used. By the results from characterization of membrane surface with FTIR, XPS, SEM and Contact angle methods show that MPC was successful modified on the SWRO membrane without defect.

Through the membrane RO filtration performance test during 30 hours compaction and 2 sets of anti-fouling test, can confirm the MPC modified membrane's performance. At compaction steps, the initial water permeate flux of the MPC modified membranes for DOW and Toray were increased both company membranes. Also, during this step, the stable rejection tendency data remained steady degree. From these results mean that the surface modification of SWRO membranes with zwitterionic chemical MPC was approximately successful with no defect on the membrane surface. In continuing step, 2 sets of anti-fouling test with two model foulants one is sodium alginate and another is bovine albumin serum, in this results, can say that when MPC modified membranes increased hydrophilicity of membrane surface, then this effect increases the membrane flux recovery efficiency with enhanced fouling resistance. Also, the potentiality when the zwitterionic chemical grafted on the SWRO membrane surface, the long-term operation is possible that applied to actual process.

Therefore, the increasing the surface hydrophilicity resulting from existence of MPC during the modified TFC SWRO membrane composite coating is believed to be a key basis for improved anti-fouling efficiency of MPC modified membrnaes. Until now, the successful surface modification of MPC on SWRO membrane surfaces is prospective opportunities for seawater desalination industrial area. Further research is needed to investigate the anti-fouling mechanism of zwitterionic hydration layer when in the seawater feed solution through optimization of the modification step and stability for test the long term stability over the modified membranes.

Reference

Inoue, Y., Onodera, Y., Ishihara, K. (2016). "Preparation of a thick polymer brush layer composed of poly(2-methacryloyloxyethyl phosphorylcholine) by surface-initiated atom transfer radical polymerization and analysis of protein adsorption resistance." *Colloids Surf B Biointerfaces* 141: 507-512.

Azuma, T., Ohmori, R., Teramura, Y., Ishizaki T., Takai, M. (2017). "Nano-structural comparison of 2-methacryloyloxyethyl phosphorylcholine- and ethylene glycol-based surface modification for preventing protein and cell adhesion." *Colloids Surf B Biointerfaces* 159: 655-661.

Azuma, T., Ohmori, R., Teramura, Y., Ishizaki, T., Takai, M. (2017). "Nano-structural comparison of 2-methacryloyloxyethyl phosphorylcholine- and ethylene glycol-based surface modification for preventing protein and cell adhesion." *Colloids Surf B Biointerfaces* 159: 655-661.

Hossain, Taslima, Alam, Mohammad A., Rahman, Mohammad A., Sharafat, Mostafa K., (2018). "Zwitterionic poly(2-(methacryloyloxy) ethyl phosphorylcholine) coated mesoporous silica particles and doping with magnetic nanoparticles." *Colloids and Surfaces A: Physicochemical and Engineering Aspects* 555: 80-87.

Chen, Jung-San,. Ting, Yi-Shao, Tsou, Hui-Ming, Liu, Ting-Yu. (2018). "Highly hydrophilic and antibiofouling surface of zwitterionic polymer immobilized on polydimethylsiloxane by initiator-free atmospheric plasma-induced polymerization." *Surface and Coatings Technology* 344: 621-625.

Wu, Chang., Chang, Weiuan, Qi, Hongzhao, Long, Lixia, Zaho, Jin, Yuan. (2017). "A facile technique for fabricating poly (2-methacryloyloxyethyl phosphorylcholine) coatings on titanium alloys." *Journal of Coatings Technology and Research* 14(5): 1127-1135.

Davenport, D. M., Lee, Jongho, Elimelech, Menachem. (2017). "Efficacy of antifouling modification of ultrafiltration membranes by grafting zwitterionic polymer brushes." *Separation and Purification Technology* 189: 389-398.

Boo, Chanhee, Elimelech, Menachem., Hong, Seungkwan. (2013). "Fouling control in a forward osmosis process integrating seawater desalination and wastewater reclamation." *Journal of Membrane Science* 444: 148-156.

Hirsch, U. Ulrike Ruehl, Macro Teuscher, Nico Hilmann, Andreas. (2018). "Antifouling coatings via plasma polymerization and atom transfer radical polymerization on thin film composite membranes for reverse osmosis." *Applied Surface Science* 436: 207-216.

Choi, Hyoungwoo, Jung, Yongdoo, Han, Sungsoo, Tak, Taemoon, Kwon, Young-Nam. (2015).

"Surface modification of SWRO membranes using hydroxyl poly(oxyethylene) methacrylate and zwitterionic carboxylated polyethyleneimine." *Journal of Membrane Science* 486: 97-105.

Shahkaramipour, Nima., Ramanan, Sankara N., Fister, David., Park, Eugene, venna, Surendar R., Sun, Haotian,. (2017). "Facile Grafting of Zwitterions onto the Membrane Surface To Enhance Antifouling Properties for Wastewater Reuse." *Industrial & Engineering Chemistry Research* 56(32): 9202-9212.

Jin, Kongjie., Qiao, Zhuhui., Wang, Shuai., Zhu, Shengyu., Cheng, Jun., Yang, Jun., Liu, Weimin (2016). "The effects of the main components of seawater on the tribological properties of Cu–9Al–5Ni–4Fe–Mn alloy sliding against AISI 52100 steel." *RSC Advances* 6(8): 6384-6394.

Zhao, D., Qiu, G., Li, X., Wan, C., Lu, K., Chung, T.S. (2016). "Zwitterions coated hollow fiber membranes with enhanced antifouling properties for osmotic power generation from municipal wastewater." *Water Res* 104: 389-396.

Kirschner, Alon Y., Chang, Chia-Chih., Kasemset, Sirirat., Emrick, Todd., Freeman, Benny D. (2017). "Fouling-resistant ultrafiltration membranes prepared via co-deposition of dopamine/zwitterion composite coatings." *Journal of Membrane Science* 541: 300-311.

Marré Tirado, Miguel Levi., Bass, Mari., Piatkovsky, Mari., Ulbricht, Mathias., Herzberg, Moshe., Freger, Viatcheslav. (2016). "Assessing biofouling resistance of a polyamide reverse osmosis membrane surface-modified with a zwitterionic polymer." *Journal of Membrane Science* 520: 490-498.

Ma, Rong., Ji, Yan-Li., Guo, Yao-Shen., Mi, Yi-Fang., An, Quan-Fu., Gao, Cong-Jie. (2017). "Fabrication of antifouling reverse osmosis membranes by incorporating zwitterionic colloids nanoparticles for brackish water desalination." *Desalination* 416: 35-44.

Shafi, Hafiz Zahid., Matin, Asif., Khan, Zafarullah., Khalil, Amjad., Gleason, Karen K. (2015). "Surface modification of reverse osmosis membranes with zwitterionic coatings: A potential strategy for control of biofouling." *Surface and Coatings Technology* 279: 171-179

Vatanpour, Vahid., Zoqi, Naser. (2017). "Surface modification of commercial seawater reverse osmosis membranes by grafting of hydrophilic monomer blended with carboxylated multiwalled carbon nanotubes." *Applied Surface Science* 396: 1478-1489.

Venault, Antoine., Wei, Ta-Chin., Shih, Hsiao-Lin., Yeh, Ching-Cheng., Chinnathambi, Arunachalam., Alharbi, Sulaiman Ali. (2016). "Antifouling pseudo-zwitterionic poly(vinylidene fluoride) membranes with efficient mixed-charge surface grafting via glow dielectric barrier discharge plasma-induced copolymerization." *Journal of Membrane Science* 516: 13-25.

Ma, Rong., Ji, Yan-Li., Weng, Xiao-Dan., An, Quan-Fu., Gao, Cong-Jie. (2016). "High-flux and fouling-resistant reverse osmosis membrane prepared with incorporating zwitterionic amine monomers via interfacial polymerization." *Desalination* 381: 100-110.

Liu, Caihong., Lee, jongho., Small, Chad., Ma, Jun., Elimelech, Menachem. (2017). "Comparison of organic fouling resistance of thin-film composite membranes modified by hydrophilic silica nanoparticles and zwitterionic polymer brushes." *Journal of Membrane Science* 544: 135-142.

Shahkaramipour, Nima., Ramanan, Sankara N., Fister, David., Park, Eugene., Venna, Surendar R., Sun, Haotian., Cheng, Chong., Lin, Haiqing. (2017). "Facile Grafting of Zwitterions onto the Membrane Surface To Enhance Antifouling Properties for Wastewater Reuse." *Industrial & Engineering Chemistry Research* 56(32): 9202-9212

Ishihara, K., Mu, M., Konno, T., Inoue, Y., Fukazawa, K. (2017). "The unique hydration state of poly(2-methacryloyloxyethyl phosphorylcholine)." *J Biomater Sci Polym Ed* 28(10-12): 884-899.

Oktay, B., Kayaman-Apohan, N., Suleymanoglu, M., Erdem-Kuruca, S. (2017). "Zwitterionic phosphorylcholine grafted chitosan nanofiber: Preparation, characterization and in-vitro cell adhesion behavior." *Mater Sci Eng C Mater Biol Appl* 73: 569-578.

Kirschner, Alon Y., Chang, Chia-Chih., Kasemset, Sirirat., Emrick, Todd., Freeman, Benny D. (2017). "Fouling-resistant ultrafiltration membranes prepared via co-deposition of dopamine/zwitterion composite coatings." *Journal of Membrane Science* 541: 300-311.

Bengani-Lutz, P, Converse, E, Cebe, P, Asatekin, A. (2017). "Self-Assembling Zwitterionic Copolymers as Membrane Selective Layers with Excellent Fouling Resistance: Effect of Zwitterion Chemistry." *ACS Appl Mater Interfaces* 9(24): 20859-20872.